3.1.6 Aerometric Measurements

Examples of the seasonal variations of the pollutant concentrations at the four test sites are given in (Figures 3-13a-d) for the monthly average values of the concentrations of NO_2 and O_3 these were found to be important factors in the damage functions for galvanized steel, nickel, and the house paints (see Section 4.0). At Burbank (Figure 3-13a) the data for the two-year exposure period showed a strong seasonal effect for O_3 which paralleled that found for the corrosion loss of galvanized steel, nickel (Figure 3-4) and the corresponding ACRMs (Figure9b). For NO_2 no clear seasonal effects were found with average concentrations between 40 and 70 pbb. At Long Beach (Figure 3-13b); astrong seasonal effect is observed for both pollutants with maxima for O_3 coinciding with minima for NO_2. At Salinas (Figure 3-13c), no significant seasonal variations of the O_3 or NO_2 concentrations were observed except for higher averages of NO_2 in October and November 1987. For the remainder of the exposure period, both pollutants had monthly average concentrations between 10 and 30 ppb. At Upland (Figure 3-13d), the seasonal variations of the two pollutant concentrations are the opposite of those observed at Long Beach (Figure 3-13b), since at Upland both O_3 and NO_2 follow the same seasonal trends whereas at Long Beach the O_3 concentration had a maximum when the NO_2 concentration had a minimum and vice versa.

The HNO_3 concentrations measured at the four sites are plotted in Figures 3-14 (a-d). The gaps in the plots represent missing data due to equipment malfunctions. The HNO_3 concentration at Burbank (Figure 3-14a) and Upland (Figure 3-14b) was generally higher in the summer with lows occurring in the December-February period. For Long Beach, such a trend was not that clear, and, at Salinas, the data appeared to be scattered uniformly throughout the year and were much lower than at the other three sites.

The higher concentrations in the summer were expected from the higher NO_x levels historically observed in the L.A. Basin (see also NO_2

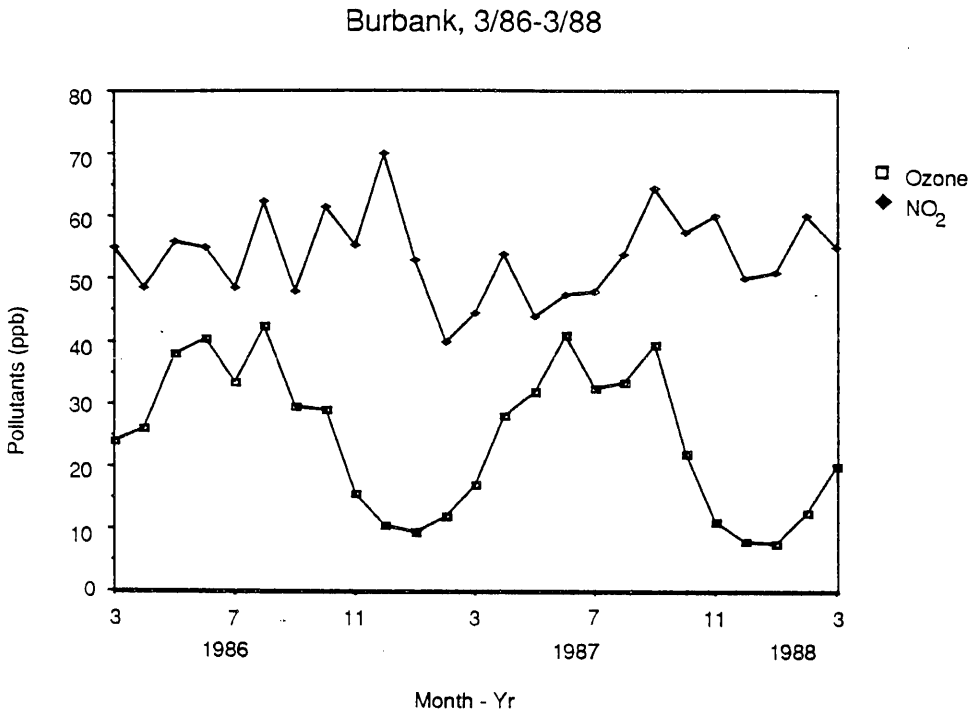

FIGURE 3-13a. BURBANK AVERAGE MONTHLY CONCENTRATIONS OF O_3 AND NO_2 FOR TWO YEAR EXPOSURE PERIOD.

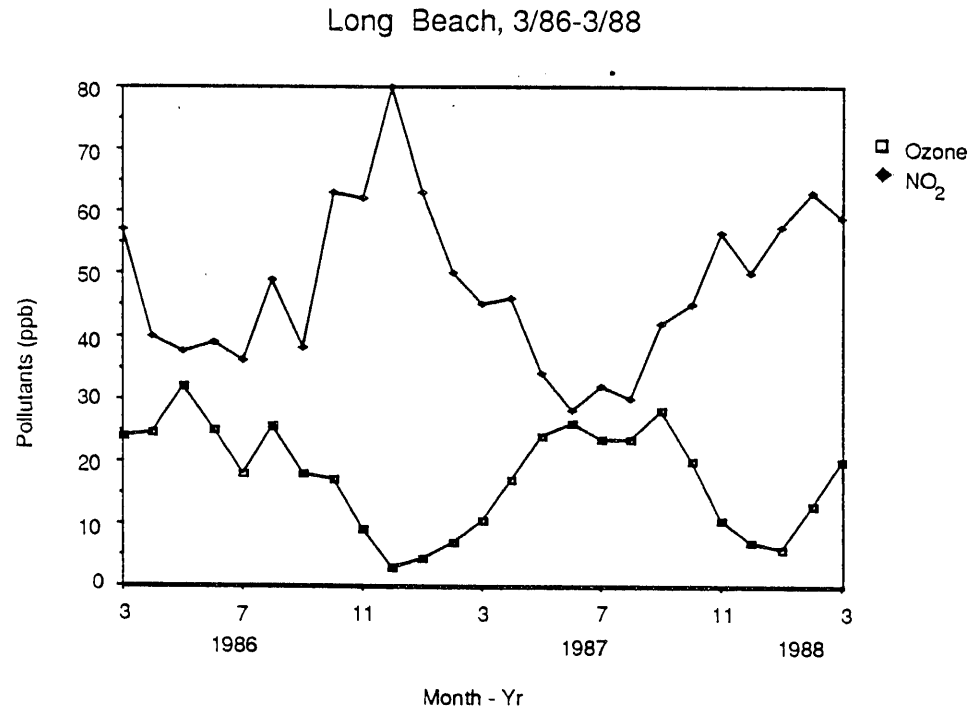

FIGURE 3-13b. LONG BEACH AVERAGE MONTHLY CONCENTRATIONS OF O_3 AND NO_2 FOR TWO YEAR EXPOSURE PERIOD.

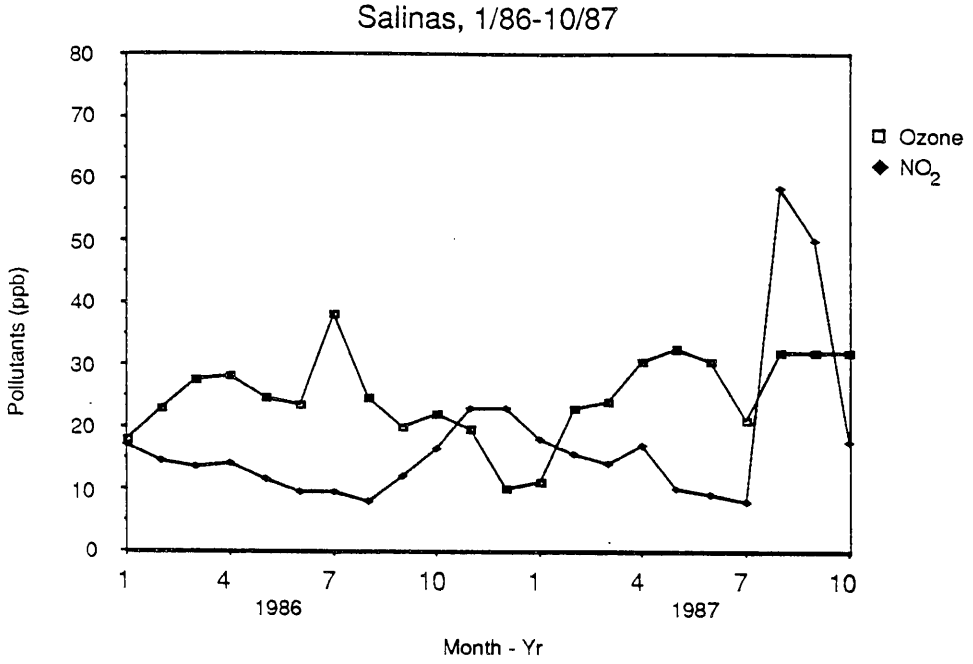

FIGURE 3-13c. SALINAS AVERAGE MONTHLY CONCENTRATIONS OF O_3 AND NO_2 FOR TWO YEAR EXPOSURE PERIOD.

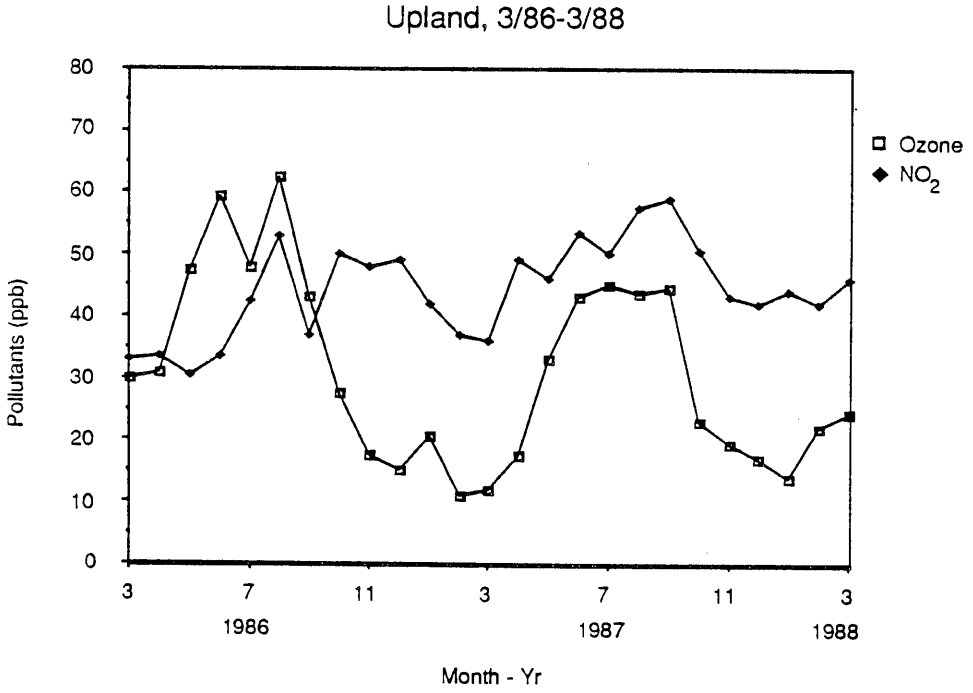

FIGURE 3-13d. UPLAND AVERAGE MONTHLY CONCENTRATIONS OF O_3 AND NO_2 FOR TWO YEAR EXPOSURE PERIOD.

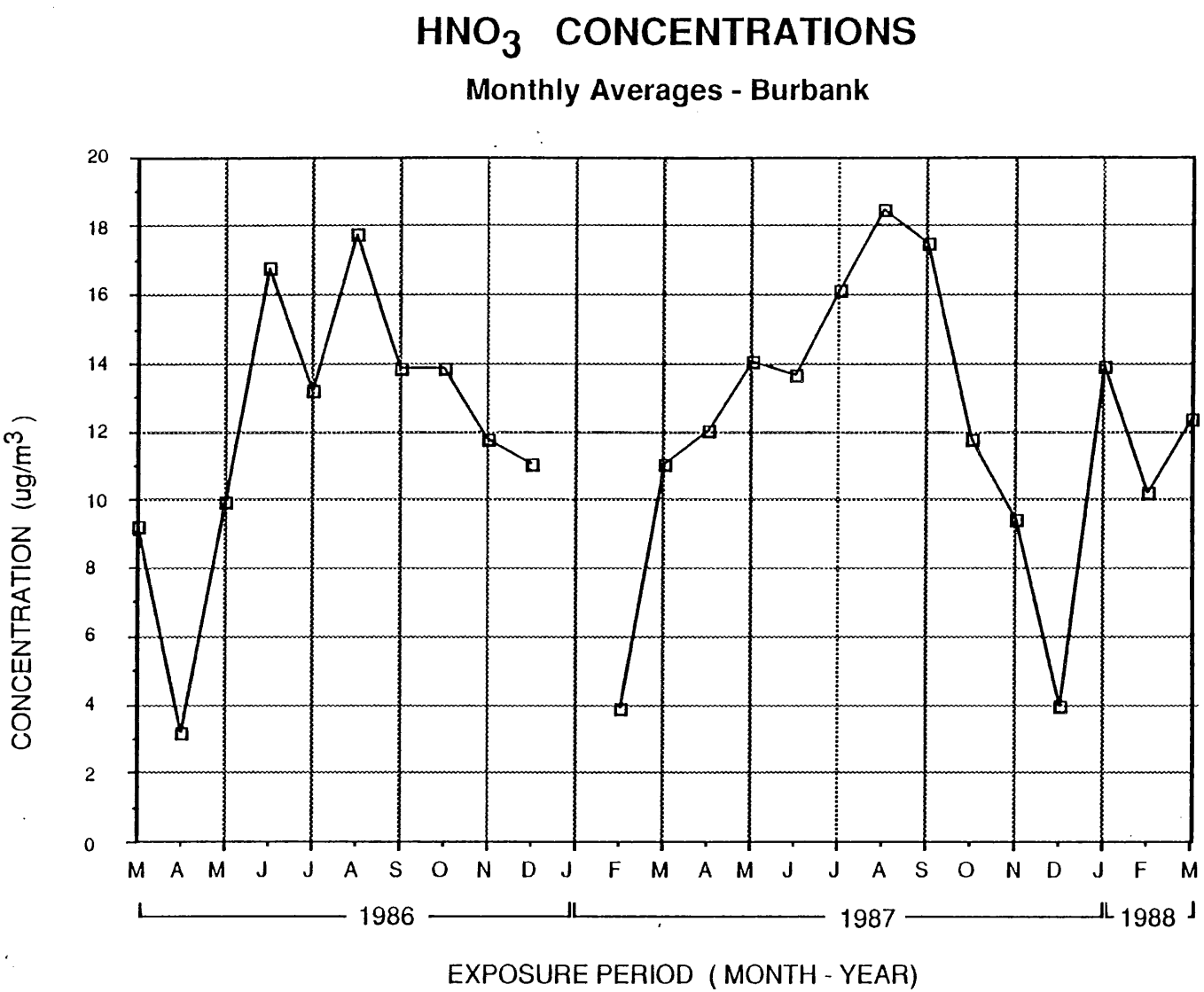

FIGURE 3-14a. AVERAGE MONTHLY HNO_3 CONCENTRATIONS FOR TWO YEAR EXPOSURE PERIOD, BURBANK SITE

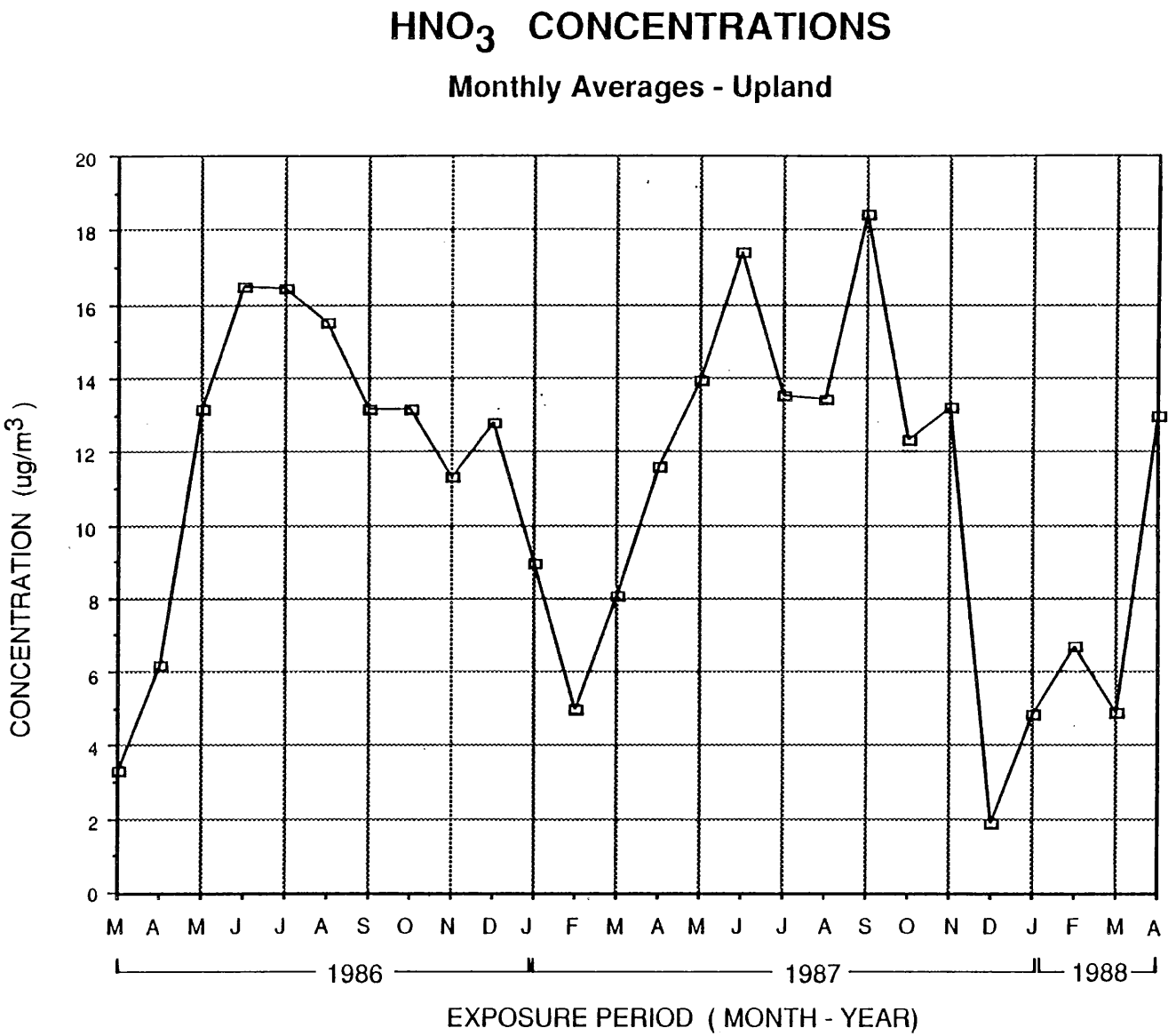

FIGURE 3-14b. AVERAGE MONTHLY HNO_3 CONCENTRATIONS FOR TWO YEAR EXPOSURE PERIOD, UPLAND SITE

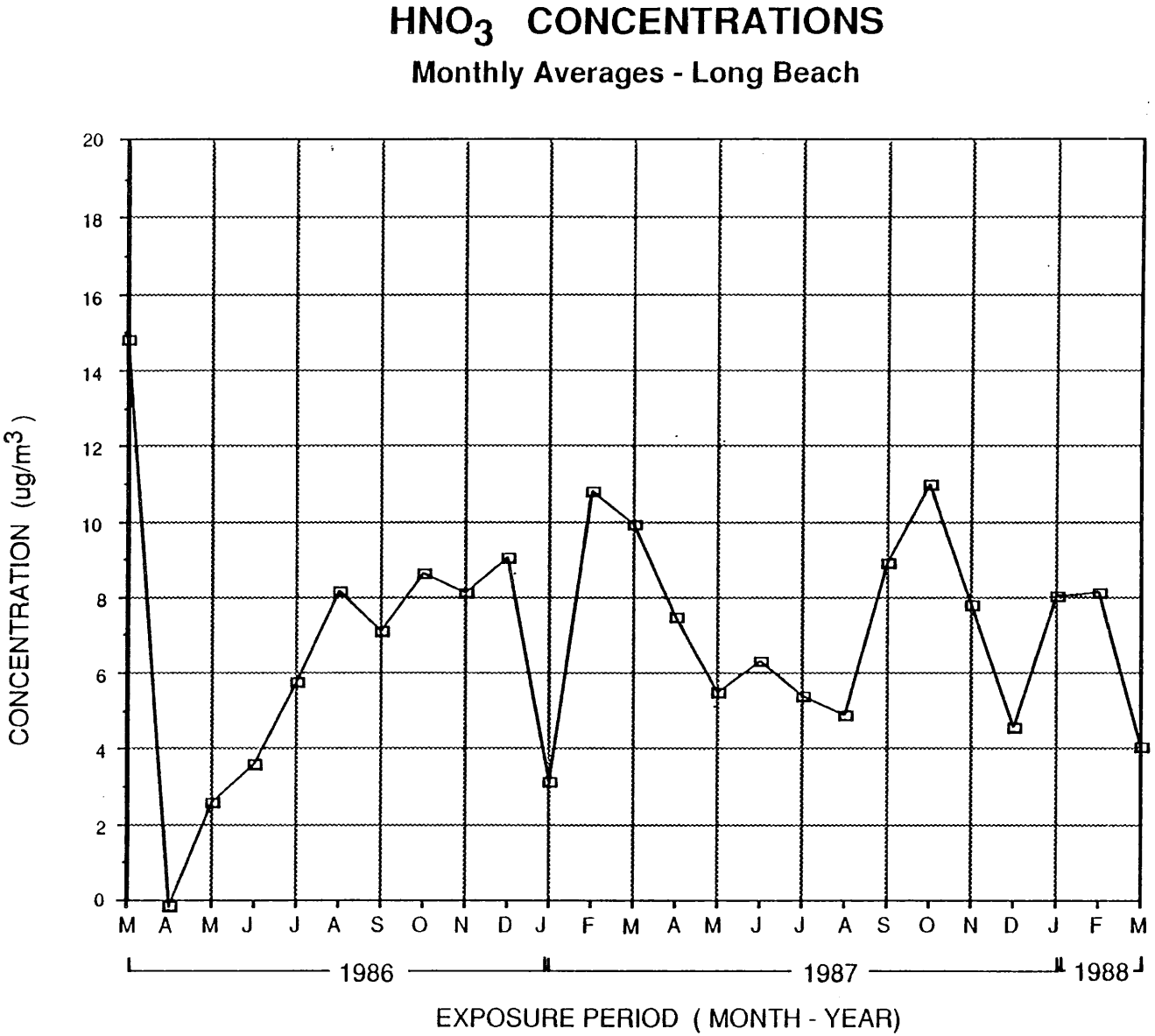

FIGURE 3-14c. AVERAGE MONTHLY HNO_3 CONCENTRATIONS FOR TWO YEAR EXPOSURE PERIOD, LONG BEACH SITE

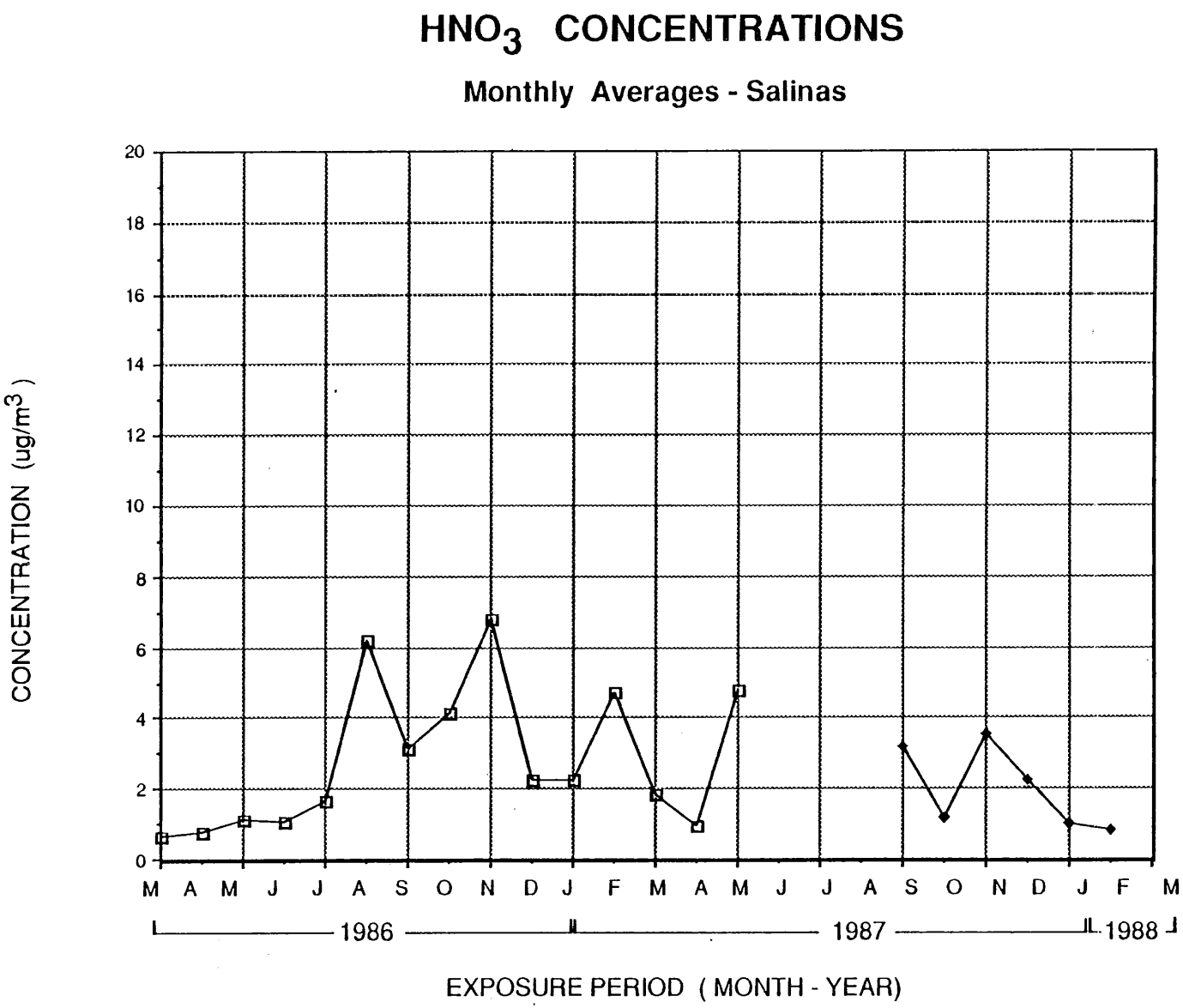

FIGURE 3-14d. AVERAGE MONTHLY HNO_3 CONCENTRATIONS FOR TWO YEAR EXPOSURE PERIOD, SALINAS SITE

data in Figure 3-13). It should be noted that these data are gross observations based on monthly averages computed from 6th day data and are not as sensitive as other measurements made by CARB using the denuder technique. The lower winter concentrations may partly account for the lower winter damage rate observed for most materials in the winter months (Section 3.1.1 - 3.1.2).

The monthly average air quality and relative humidity data for the field sites are compared in Figures 3-15 through 3-19. These figures are plots of the data used to derive the damage functions given in Section 4.0; as such, these averages are not the same as those calculated from the full set of aerometric data (Figure 3-13) because days with missing corrosion sensor (ACRM) data were excluded from the damage function database. The differences in the monthly averages were small.

Figure 3-15 shows that there was a large variation in the concentration of SO_2 between the sites, as was intended in the project (see Section 2.0). The Long Beach site experienced relatively high SO_2 levels because of the proximity of sources including petrochemical industries, ships in the harbor, and large electricity generating stations. Burbank had the next highest SO_2 levels, followed by Upland and Salinas, which had virtually undetectable levels. The seasonal pattern in Long Beach and Burbank was the same, with strong peaks in the winter coinciding with cold stagnation periods, and possibly, when utilities switched from gas to oil during cold weather because of high residential demand for natural gas. There was a second peak in August 1986 which was probably caused by a hot period with unusually high electrical demand.

The seasonal patterns for NO_x, given in Figure 3-16, are similar to those of SO_2, also a primary pollutant. The wintertime peak was especially pronounced at Long Beach and Burbank. Upland showed little seasonal variation. Salinas had a clear wintertime peak, but the levels were much lower than those in the South Coast Air Basin (SCAB).

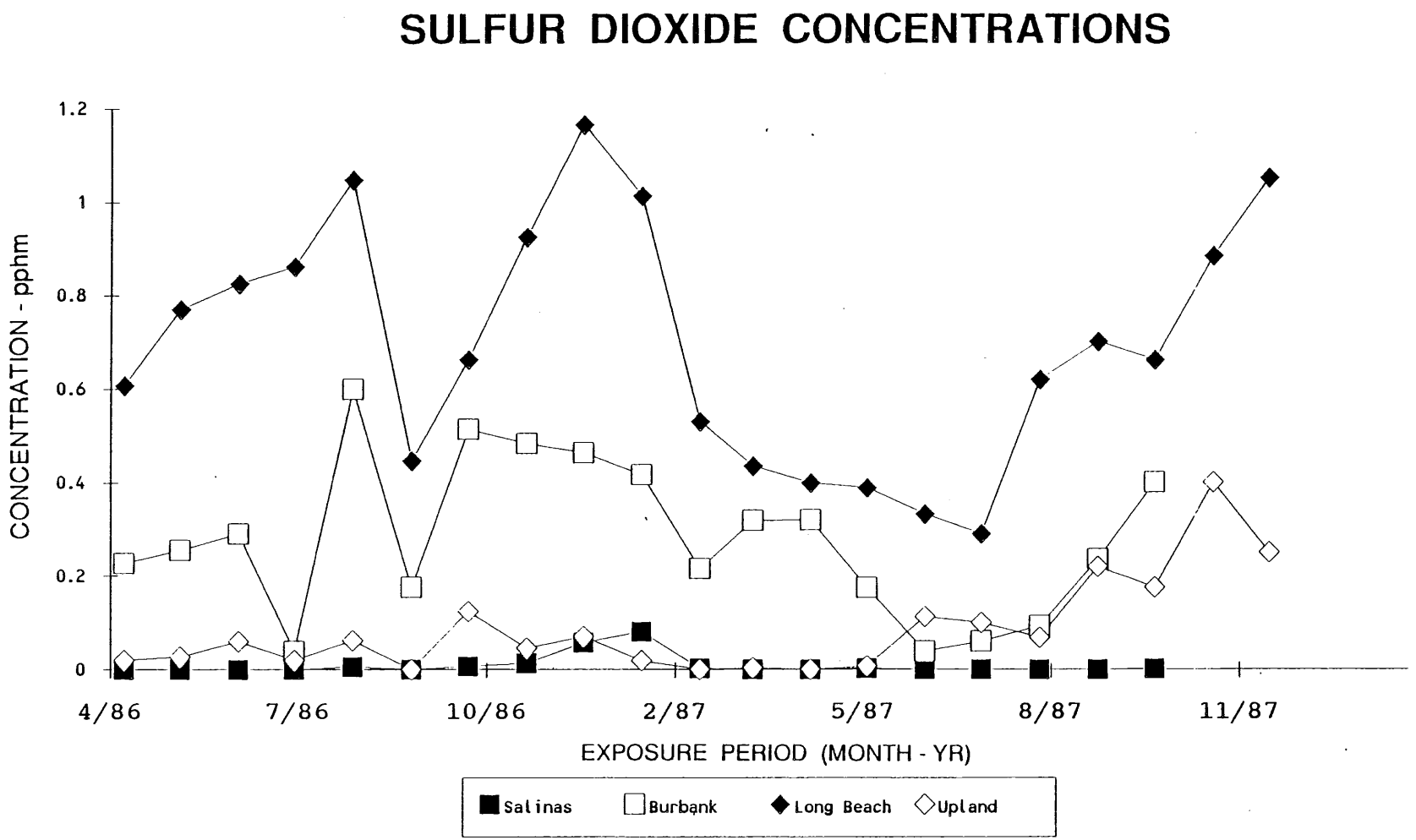

FIGURE 3-15. MONTHLY AVERAGE SULPHER DIOXIDE LEVELS

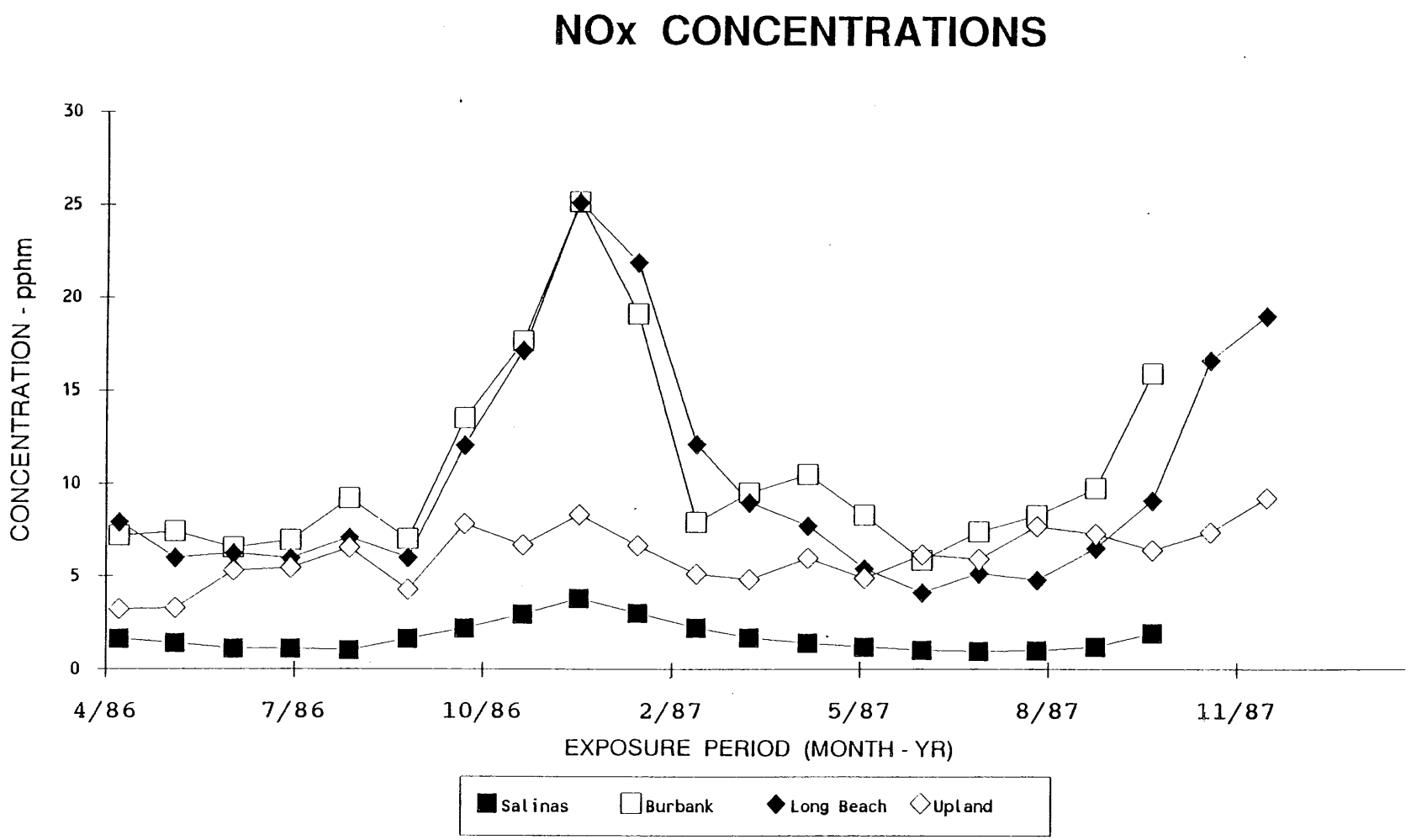

FIGURE 3-16. MONTHLY AVERAGE NO_X LEVELS

As a secondary pollutant formed by the action of sunlight on precursor gases in the atmosphere, O_3 has a completely different seasonal pattern than the two primary pollutants discussed above. Figure 3-17 gives the monthly average O_3 levels at all the sites. The strong summertime peak and the wintertime minimum were evident at all sites. Upland had the highest levels since it is downwind of the large emissions of precursors in the L.A. basin. However, there was not as great a difference in concentrations between the sites as with other pollutants since O_3 is formed by photochemical chain reactions in the atmosphere which are non-linearly related to the emissions of the precursors.

Corrosion requires the presence of sufficient humidity to make the reactions possible. Two humidity variables are plotted in Figures 3-18 and 3-19. T60 is the fraction of the day during which the relative humidity was greater than or equal to 60% (Figure 3-18). The coastal site at Long Beach had the highest relative humidity with Burbank and Upland being quite similar to each other. As discussed in Section 3.1.4, Salinas had insufficient valid relative humidity data. There was a mild trend toward higher humidities in the summer and fall (Figure 3-19).

Corrosion rates as measured by weight loss, strength loss, and indicated by the ACRM data showed a strong increase in the summer (see 3.1.1 - 3.1.3). This was surprising since the primary pollutants peak so strongly in the winter and there was not a large difference in relative humidity between winter and summer that could explain the observed difference in corrosion behavior. Also, O_3 itself did not cause significant damage to metals in the laboratory tests (see 3.2). The only reasonable inference is that certain components of photochemical smog are the main causes of corrosion in California. The most likely species are HNO_3 vapor, SO_4^{-2}, NO_3^- and organic acid airborne particles.

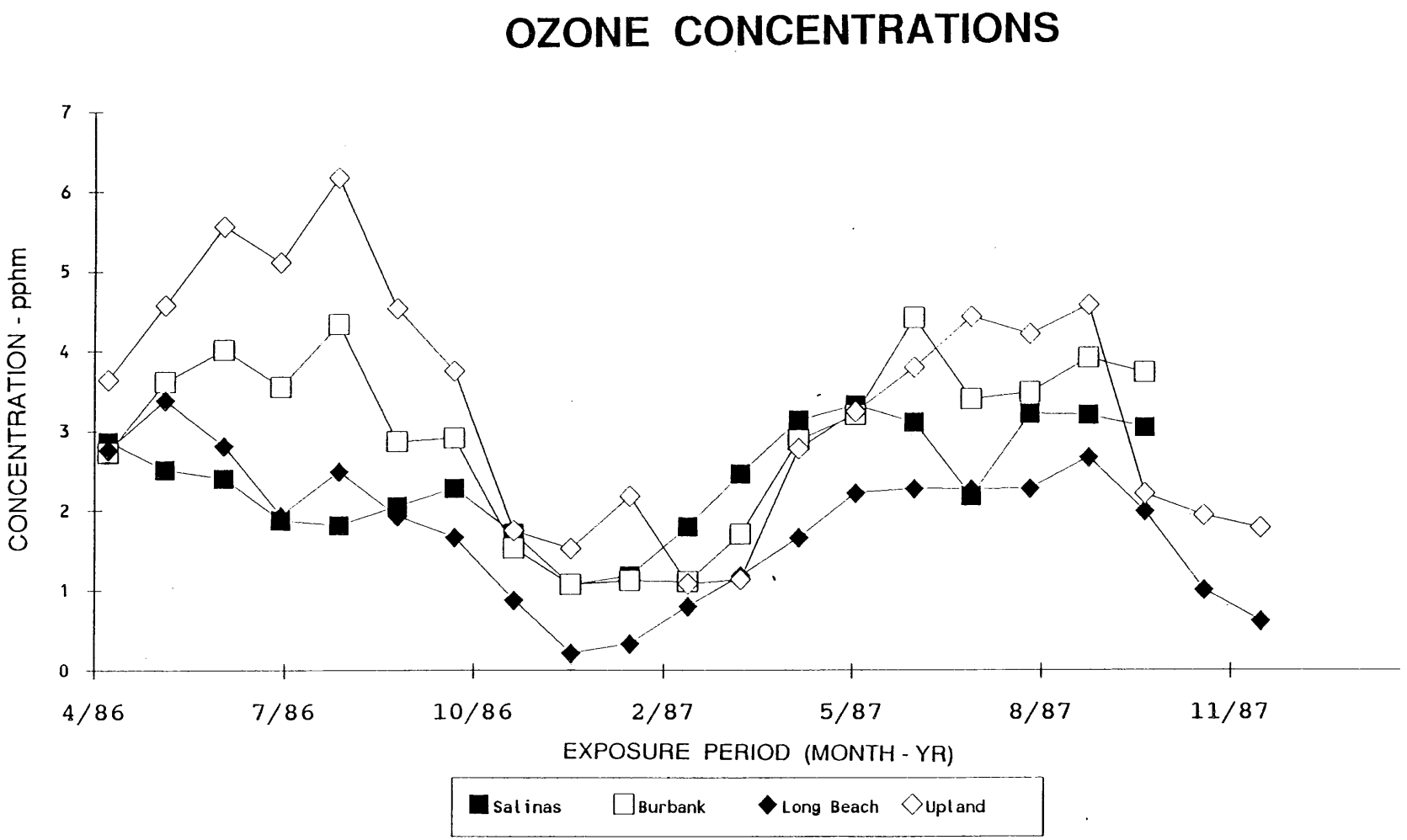

FIGURE 3-17. MONTHLY AVERAGE OZONE LEVELS

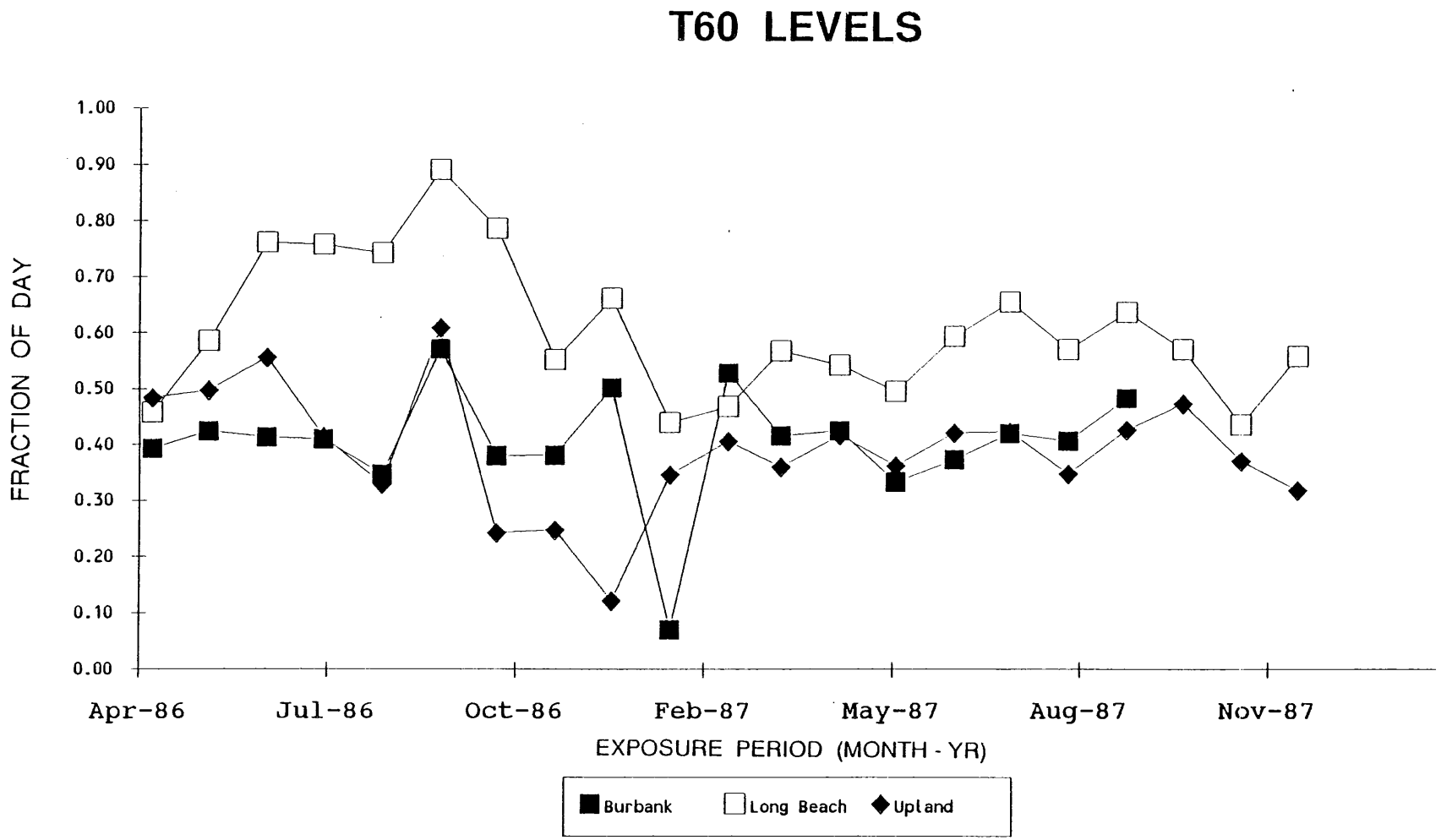

FIGURE 3-18. MONTHLY AVERAGE T60 VALUES.

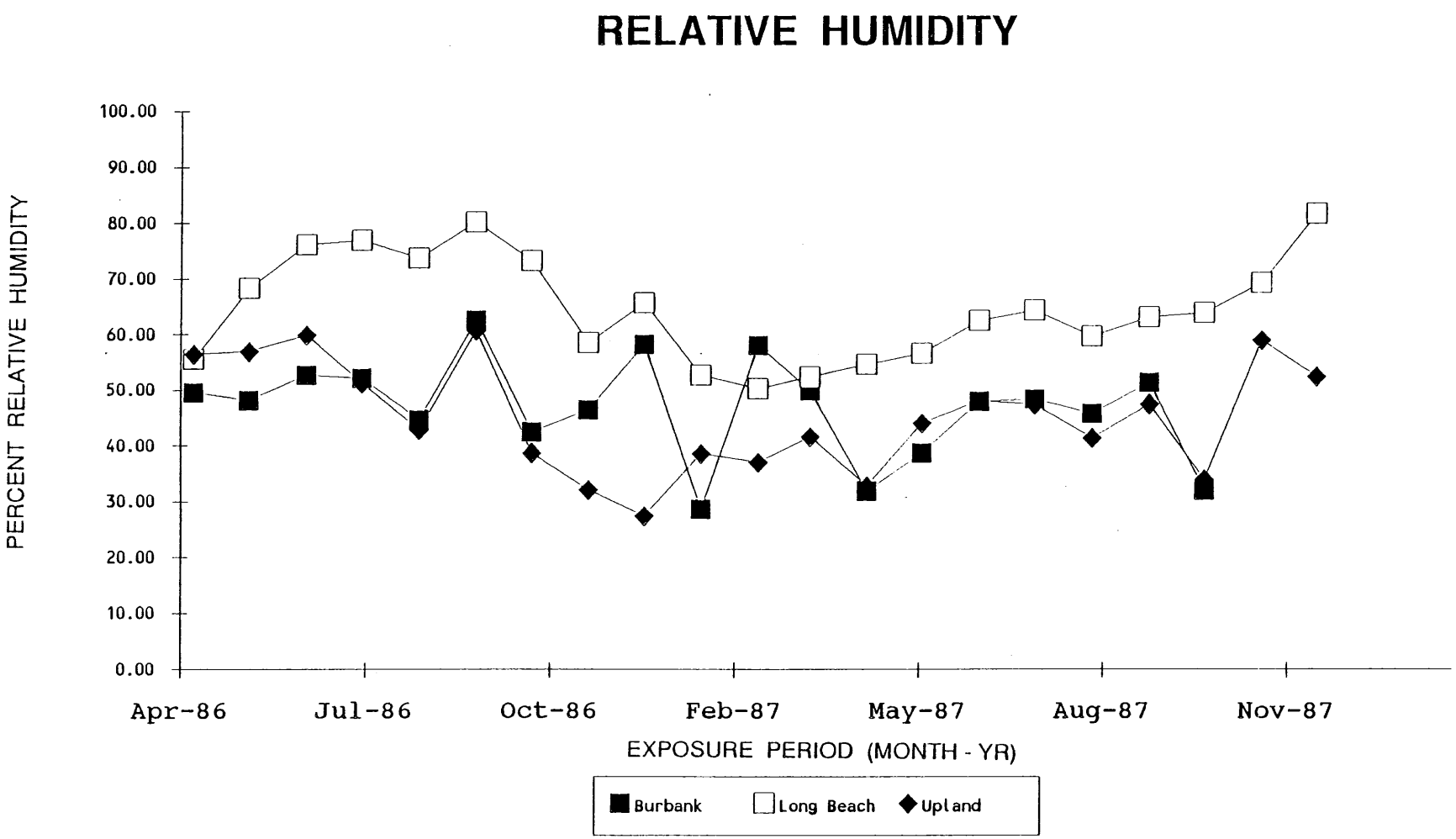

FIGURE 3-19. MONTHLY AVERAGE PERCENT RELATIVE HUMIDITY

3.2 LABORATORY TESTS

In the following, the data obtained at the Rockwell International Science Center (SC) will be included in the discussion of the experimental results. Details of this part of the work have also been given in a previous report (Jeanjaquet, 1988). The materials exposed in the SC series were galvanized steel, nickel, and the two house paints previously described. Not all tests in the first test matrix were completed at SC, tests SC 5, 9, and 10 were carried out at CEEL/USC under this project. The USC test series consists of tests USC 1-8. Table 3-2 lists the test conditions for both test series. In addition to the four materials exposed in the SC series, bare aluminum, textile (nylon) and paint on wood were also tested.

3.2.1 Coupon Exposure

Corrosion damage was determined by EMSI personnel using weight loss methods for galvanized steel, nickel, aluminum, and the two paints. For the textile samples, mechanical tests were performed at Purdue University for the textile samples. Weight loss data for aluminum were only available for tests USC 3-8. Corrosion damage to paint on wood was determined by an appearance measurement method as discussed in Section 3.1.4. No quantitative results could be obtained in this case.

Table 3-3 gives a summary of the results of the damage measurements. Tests SC 1 and 2 were carried out at RH = 90%. Since very high corrosion rates were observed in test SC 2 (1 ppm SO_2), it was decided to reduce RH to 80% for the remainder of the program. For tests SC 2-7 and SC 9 the pollutant concentration was 1 ppm, for the other tests (except SC 1 and USC 2, which were blanks without pollutants) the pollutant concentration was 0.5 ppm. The tests in the presence of 0.5 ppm SO_2 and 0.5 ppm NO_2 were repeated three times (SC 10, USC 1 and 7) in order to check the reproducibility of the results. Problems with determination of weight loss for galvanized steel occurred in tests USC 5-8, which made it necessary to use a different descaling technique (see

TABLE 3-2. CONDITIONS FOR TEST SERIES AT ROCKWELL INTERNATIONAL SCIENCE CENTER (SC) AND UNIVERSITY OF SOUTHERN CALIFORNIA (USC)

Test #	RH (%)	Pollutants	Aerosol
SC 1	95	none	
SC 2	95	1 ppm SO_2	
SC 3	80	1 ppm O_3	
SC 4	80	1 ppm SO_2	
SC 5*	80	1 ppm NO_2	
SC 6	80	1 ppm each SO_2, NO_2, O_3	
SC 7	80	1 ppm each SO_2, NO_2, O_3	H_2SO_4
SC 8	80	1 ppm each SO_2, NO_2, O_3	HNO_3
SC 9*	80	1 ppm each SO_2, NO_2	
SC 10*	80	0.5 ppm each SO_2, NO_2	
USC 1	80	0.5 ppm each SO_2, NO_2	
USC 2	80	none	
USC 3	80	0.5 ppm NO_2	
USC 4	80	0.5 ppm each SO_2	
USC 5	80	none	0.1 ppm HNO_3
USC 6	80	none	0.5 ppm HNO_3
USC 7	80	0.5 ppm each SO_2, NO_2	
USC 8	80	none	0.5 ppm HNO_3 (4 L/min)

NOTE: * Tests carried out at USC

TABLE 3-3. WEIGHT LOSS DATA FOR LABORATORY TESTS (MG / 155 CM^2 IN 28 DAYS) AND LOSS OF STRENGTH (%) FOR NYLON TEXTILE.

Test #	Galv. Steel	Ni	CF Paint	C Paint	Al	Textile
SC 1	-3.6 ± 2.8	15.3 ± 17.6	3.9 ± 3.1	-5.6 ± 1.5		
SC 2	6.6 ± 0.7	46.4 ± 13.9	41.7± 5.8	14.0 ± 0.1		
SC 3	-11.2 ± 1.2	10.0 ± 10.2	15.9 ± 8.3	-1.2 ± 1.7		
SC 4	42.7 ± 2.9	165.4 ± 10.2	25.0 ± 1.9	0.3 ± 0.1		
SC 5*	3.1 ± 11.9	4.0 ± 0.5	6.3 ± 0.4	2.4 ± 0.1		
SC 6	111.5 ± 6.5	12.0 ± 5.2	21.3 ± 5.2	42.0 ± 2.0		
SC 7	n.d.	n.d.	n.d.	n.d.		
SC 8	619.4 ± 67.0	233.5 ± 24.5	55.0 ± 4.5	311.1 ± 13.5		
SC 9*	45.8 ± 0.4	127.2 ± 23.2	4.2 ± 1.0	-1.0 ± 1.4		
SC 10*	59.2 ± 12.7	168.5 ± 2.8	4.3 ± 0.1	34.2 ± 0.6		
USC 1	35.8 ± 9.7	158.0 ± 30.0	1.7 ± 0.2	5.0 ± 1.2	n.d.	2.1 ± 0.7
USC 2	-11.5 ± 3.1	-1.8 ± 0.1	1.5 ± 1.3	10.0 ± 1.7	n.d.	-2.0 ± 0.4
USC 3	-15.4 ± 2.0	-0.8 ± 0.4	11.1 ± 8.5	8.6 ± 0.6	0.4 ± 0.1	-2.6 ± 0.6
USC 4	31.2 ± 7.4	165.0 ± 0.6	7.5 ± 4.9	6.5 ± 1.5	1.2 ± 0.1	-1.9 ± 1.1
USC 5	-19.8 ± 4.0	2.8 ± 1.3	4.2 ± 0.1	2.9 ± 0.2	2.9 ± 0.5	5.7 ± 0.4
USC 6	19.3 ± 7.7	19.8 ± 0.3	12.1 ± 4.3	37.2 ± 6.7	22.8 ± 2.3	14.7 ± 0.8
USC 7	11.7 ± 7.9	33.5 ± 3.0	7.6 ± 0.1	88.3 ± 2.9	0.9 ± 0.3	0.8 ± 1.0
USC 8	2.4 ± 5.6	1.1 ± 0.8	7.6 ± 1.5	95.5 ± 7.5	4.3 ± 0.8	3.6 ± 4.8

NOTE: *run at USC negative values correspond to a weight gain or increase of fiber strength
n.d.: no data

the Appendix). The weight loss data are subject to considerable uncertainty.

In the SC tests involving aerosols (SC 7 and 8) no weight loss data were available for test SC 7. For test SC 8 the HNO_3 concentration was too high; these data should be disregarded. Tests USC 6 and 8 were used. Test USC 5 was carried out at 0.1 ppm HNO_3. During September 26-27, 1988, John Horrocks of ARB/El Monte, California, sampled for HNO_3 at the test chamber. His results and conclusions were as follows:

"Three samples were collected both at the inlet and outlet to the chamber. The 95% confidence range for concentrations at these locations (mean $\pm$2 standard deviations) were:

Inlet: 2.54 ± 0.53 ppm
Outlet: 0.35 ± 0.09 ppm

The anticipated concentration was 0.50 ppm. These results indicate a large gradient between the inlet and outlet. The observed gradient is perhaps not too surprising in view of the observed condensation in the chamber at the air inlet, where most of the drop in concentration probably occurs. Since I did not sample inside the chamber, I cannot determine the concentration at which materials are exposed, but I suspect it is closer to the measured outlet concentration than to the inlet concentration."

A qualitative evaluation of the results in Table 3-3 shows that for zinc and nickel significant corrosion rates occurred only in the presence of SO_2. For a 28-day test with a sample of 155 cm^2 (one side exposed), a corrosion rate of 1 um/yr corresponds to a weight loss of 8.5 mg for zinc and 10.5 mg for nickel. These values were exceeded for galvanized steel and nickel only in those tests which included SO_2 as a pollutant. It was initially surprising that NO_2 had no effect on the corrosion behavior of zinc and nickel. However, monitoring of the SO_2 and NO_2 concentrations at the outlet of the test chamber showed that the

SO_2 concentration decreased immediately when the coupon surface was chilled, but the NO_2 concentration remained constant (Figure 3-20). This result suggests that most of the SO_2 is dissolved in the surface film which forms when the sample is chilled, while NO_2 does not dissolve under the same circumstances. For the HNO_3 aerosol tests (USC 5, 6, and 8) an increase of corrosion rates with increasing HNO_3 concentration was observed for all materials studied. Lowering the flow rate to 4 l/min. (test USC 8) reduced corrosion rates significantly for all materials except the carbonate extender containing paint.

In the USC tests bare aluminum and textile (nylon fabric) were also exposed (Table 3-3). For aluminum, weight loss data were not obtained in USC 1 and 2. The results for the three tests involving HNO_3 aerosol showed that increasing the aerosol concentration accelerated corrosion and that reducing the flow rate reduces the corrosion rate. Similar results were obtained for the nylon fabric, the corrosion behavior of which was characterized by loss of strength in Table 3-3. In the absence of pollutants (USC 2), the presence of NO_2 (USC 3) and in the presence of SO_2 (USC 3) no loss of strength was observed.

Since RH plays an important role in the atmospheric corrosion process, it was attempted to keep RH as close as possible to 80%. However, the RH-sensors exposed in the test's chamber were not as reliable as expected and their performance degraded with increasing exposure to the pollutants. Some variation in the test results was undoubtedly due to this problem.

3.2.2 ACRM Exposure

The results of the ACRM exposure in the laboratory tests including those obtained at SC are given in Table 3-4. The data for t_{corr} and INT are the averages for two zinc and two nickel sensors, respectively. The units of INT in Table 3-4 are 10^{-3}msec/ohm for 12 hour periods, since INT is obtained every 12 hours from integration of the $1/R_p(ohm^{-1})$ versus time(sec) curves.

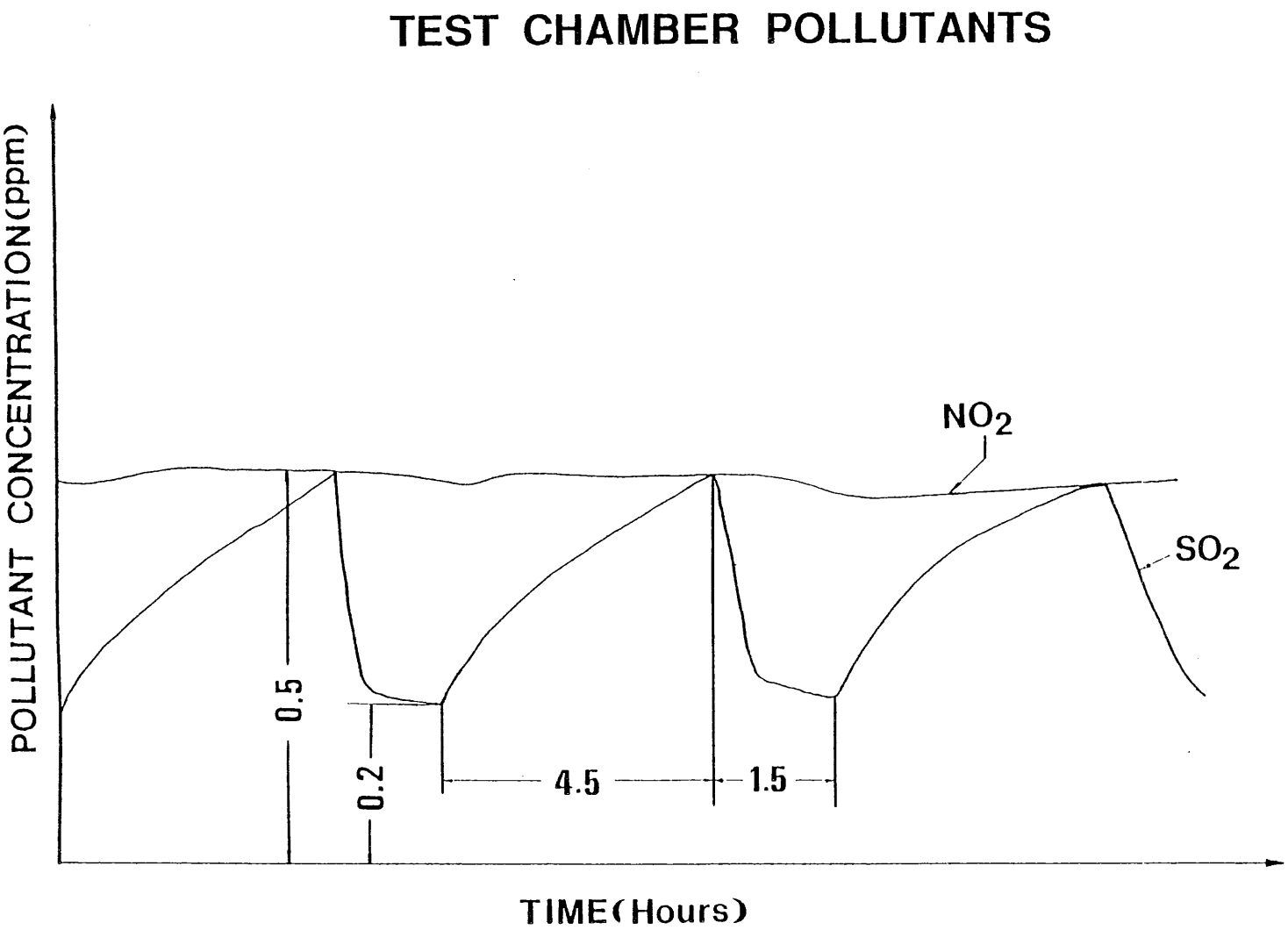

FIGURE 3-20. TEST CHAMBER OUTPUT CONCENTRATIONS OF SO_2 AND NO_2

TABLE 3-4. SUMMARY OF ACRM DATA – LABORATORY TESTS (SC AND USC SERIES)

(t_{70}, t_{80}, t_{corr}, in h/day; Int in 10^{-3} sec/ohm for a 12h period; average of two ACRMs for each metal)

Test #	t_{70}	t_{80}	t_{corr},Zn	t_{corr},Ni	Int,Zn	Int,Ni
SC1	24	23.96	4.33±0.32	4.52±1.35	4.79±2.60	7.05±5.55
SC2	24	23.92	21.09±0.59	22.95±0.81	241.4±227.7	284.3±53.4
SC3	24	16.3	5.92±0.01	6.37±0.13	1.28±1.06	2.57±0.07
SC4	24	1.14	14.27±8.19	18.62±5.18	85.9±83.7	54.4±29.8
SC5	24	0	2.59±0.78	5.75±0.49	1.14±1.03	2.30±0.01
SC6	24	0.13	9.04±1.42	20.30±2.53	5.31±1.24	87.2±33.7
SC7	24	4.6	13.30±6.10	20.60±0.15	176.1±175.8	51.9±11.0
SC8	24	7.0	23.52±0.46	23.86±0.11	1738±899.3	2766±2502.0
SC9[+]	24	15.3	4.5±2.8	4.3±1.9	5.24±4.70	3.63±1.12
SC10[+]	24[*]	15.7[*]	8.3±1.3	2.3±0.1	76.18±16.93	2.77±1.38
USC1	n.d.	n.d.	0.009±0.003	11.5±9.5	0.35±0.06	103.7±102.3
USC2	18.6	8.5	0.3±0.3	0.0	0.71±0.16	5.91±0.03
USC3	23.9	6.84	0.14±0.14	0.04±0.04	1.27±0.78	0.38±0.02
USC4	23.8[*]	12.7[*]	4.92±1.40	7.94±5.79	26.2±0.0	83.2±79.6
USC5	24	14.2	1.08±0.05	1.59±1.30	1.45±0.29	0.42±0.37
USC6	23	22.5	4.66±2.22	19.68±2.07	4.8±1.3	71.9±56.4
USC7	21.4	4.34	2.3±2.3	2.8±2.8	5.2±4.6	2.7±2.5
USC8	18.3	0.39	0.34±0.01	5.46±3.04	0.61±0.09	5.9±0.16

[+] Carried out at CEEL/USC
[*] First week data only

In previous applications (5-9), the ACRM surface had been pretreated in order to increase its sensitivity. This pretreatment consisted of applying a thin layer of deionized water or very dilute NaCl and some alcohol to the clean sensor surface and allowing the surface to dry. The resulting thin layer of corrosion products provided the possibility of condensation of moisture even at the early stages of exposure or under conditions of low RH. In this project, pretreatment was omitted since it was desired that the air have only the pollutants introduced in each test react with a clean sensor surface. The drawback of this approach was that the corrosivitity of the atmospheres was very low in most tests. It was possible, therefore, that one or two sensors of each material did not react sufficiently to provide a current to pass between the electrode finger as can be seen in Table 3-4, in tests SC2 for zinc and USC 1 for nickel. In the analysis of this data, only the high INT value was considered.

It is interesting to note that the t_{corr} values for the nickel ACRM were in most cases higher than those for the zinc sensor, suggesting that the particular chemistry of the corrosion products lead to longer times on nickel during which corrosion was possible. This result also showed that time-of-wetness data based solely on RH cannot give accurate data for the true time-of-wetness of a particular metal surface.

In fact, for two different metals, corrosion might occur for different lengths of time even under identical conditions. The INT data reflected the higher t_{corr} values for nickel to some extent. However, a lot of scatter was observed for the corrosion loss INT for two identical sensors despite special efforts to ensure uniform distribution of the pollutant gases in the test chamber. The main problem with the use of the ACRM's in this study was that in most cases, corrosion rates were very low, leading to minimal amounts of corrosion products covering the sensor surface. The chance that these corrosion products bridged two or more of the sensor fingers in the same manner for both sensors became much less under these circumstances than for exposure under more corrosive conditions. The results for tests SC 10, USC 1, and USC 7

illustrate this problem.

A comparison of the results obtained in the two tests at RH = 95% clearly shows that in the presence of 1 ppm SO_2 sufficient amounts of corrosion products are formed in a short time to produce t_{corr} data in excess of 20 h/day for both nickel and zinc. In this corrosive environment, corrosion rates were very high and the sensor surfaces were covered with visible layers of corrosion products in a very short time. Lowering RH to 80% (SC 4) greatly reduced t_{corr} and INT (Table 3-4). The significant effect of RH can be seen by comparing the results for tests SC 1, 3, and 5, where INT was lower in the presence of 1 ppm NO_2 (SC 5) and 1 ppm O_3 (SC 3) than in the test with RH = 95% without pollutants (SC 1) for both zinc and nickel. These and similar results for other tests shown in Table 3-4 demonstrate the usefulness of the information which can be extracted from the ACRM data.

3.2.3 Statistical Analysis

3.2.3.1 Analysis of Weight Loss Data

The purpose of the analysis was to (a) estimate the random error in the results, (b) determine which conditions caused material damage in excess of the random error in the study, (c) determine if certain combinations of pollutants caused enhanced material damage over that expected from each pollutant separately, and (d) determine if increased damage was associated with increased dosage.

The method used to answer these questions was a one-way analysis of variance of the weight loss data in Table 3-3. Experiments SC 1 and SC 2 were not included in the analysis since they were carried out at a higher relative humidity than the other experiments. Experiment SC 7 did not have weight loss data, and in experiment SC 8 the HNO_3 concentration was too large. Thus, both these tests were also excluded from the analysis.

The results of the statistical analysis are seen in Tables 3-5 through 3-10. One-way analysis of variance uses all the observations to make a combined estimate of the random error in a series of experiments carried out under different conditions. The errors are assumed to have a common normal distribution for each experiment. Under this assumption, a 95% confidence interval can be calculated for the mean damage seen in each experiment. If this interval contains zero, then the damage is not statistically significant. Similarly, if the 95% confidence interval does not include zero, the damage is statistically significant.

The means of two experiments can also be compared using the 95% confidence intervals. If the confidence intervals for two means overlap, they are not significantly different; if they do not overlap, then they are significantly different.

In interpreting these results one must remember that a finding of no significant effect does not mean that there was no effect, only that the effect was less than the random error inherent in the experimental conditions. The results for each material are discussed in detail below. A summary of the statistical analysis is given in Table 3-11.

For galvanized steel, the following conclusions are supported by the statistical analysis in Table 3-5. O_3, NO_2, and HNO_3 by themselves did not significantly increase corrosion rates while exposure to SO_2 always resulted in statistically significant damage. The effects of SO_2 was not enhanced by NO_2, but O_3 accelerated corrosion due to SO_2 in the presence of NO_2 (Test #SC6).

For nickel, as with galvanized steel, corrosion occurred only in the presence of SO_2, as shown in Table 3-6. The effect of SO_2 was not enhanced by the presence of NO_2 or O_3.

As seen in Table 3-7, the corrosion data for paint free of carbonate extender had significantly lower random errors than those for

TABLE 3-5. ONE - WAY ANALYSIS OF VARIANCE OF WEIGHT LOSS FOR GALVANIZED STEEL.

ANALYSIS OF VARIANCE

SOURCE	DF	SS	MS	F	p
FACTOR	11	31521	2866	12.63	0.000
ERROR	16	3630	227		
TOTAL	27	35151			

EXPERIMENT	N	MEAN
SC 3	2	-11.20
SC 4	2	42.70
SC5	2	3.10
SC6	2	111.50
SC 9	2	45.80
USC2	2	-11.50
USC3	2	-15.40
USC4	2	31.20
USC5	2	-19.80
USC6	2	19.30
USC8	2	2.40
SC10,USC1,7	6	35.57

RANDOM ERROR = 15.06

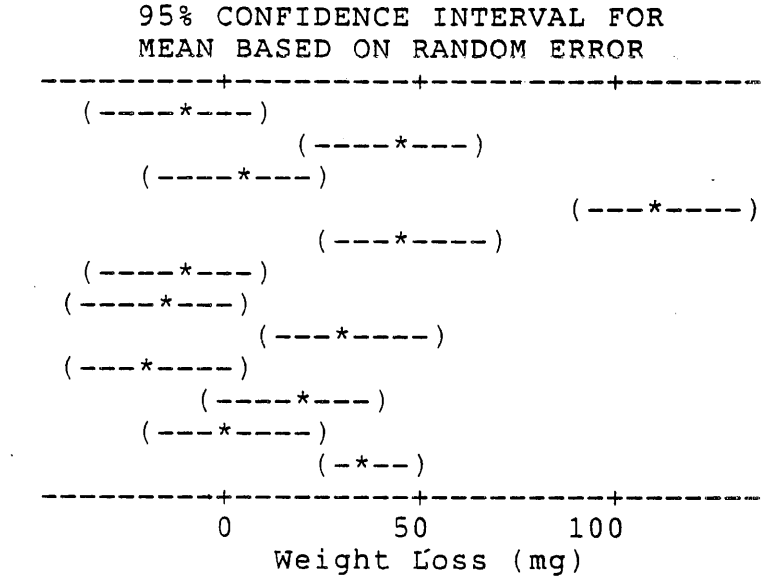

TABLE 3-6. ONE - WAY ANALYSIS OF VARIANCE OF WEIGHT LOSS FOR NICKEL.

ANALYSIS OF VARIANCE

SOURCE	DF	SS	MS	F	p
FACTOR	11	122555	11141	6.85	0.000
ERROR	16	26020	1626		
TOTAL	27	148576			

EXPERIMENT	N	MEAN
SC 3	2	10.00
SC 4	2	165.40
SC5	2	4.00
SC6	2	12.00
SC 9	2	127.20
USC2	2	-1.80
USC3	2	-0.80
USC4	2	165.00
USC5	2	2.80
USC6	2	19.80
USC8	2	1.10
SC10,USC1,7	6	120.17

RANDOM ERROR = 40.33

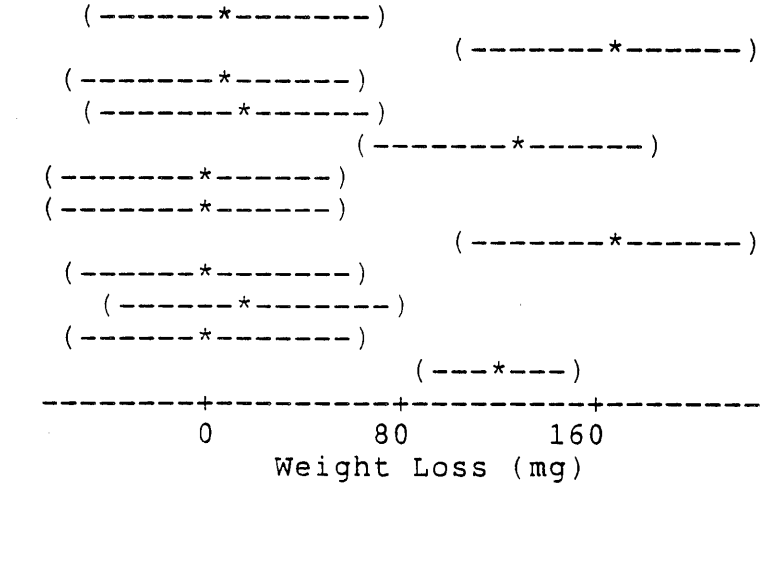

TABLE 3-7. ONE - WAY ANALYSIS OF VARIANCE OF WEIGHT LOSS FOR PAINT WITHOUT CARBONATE EXTENDER.

ANALYSIS OF VARIANCE

SOURCE	DF	SS	MS	F	p
FACTOR	11	1282.6	116.6	3.94	0.007
ERROR	16	473.9	29.6		
TOTAL	27	1756.5			

EXPERIMENT	N	MEAN
SC 3	2	15.900
SC 4	2	25.000
SC5	2	6.300
SC6	2	21.300
SC 9	2	4.200
USC2	2	1.500
USC3	2	11.100
USC4	2	7.500
USC5	2	4.200
USC6	2	12.100
USC8	2	7.600
SC10,USC1,7	6	4.533

RANDOM ERROR = 5.442

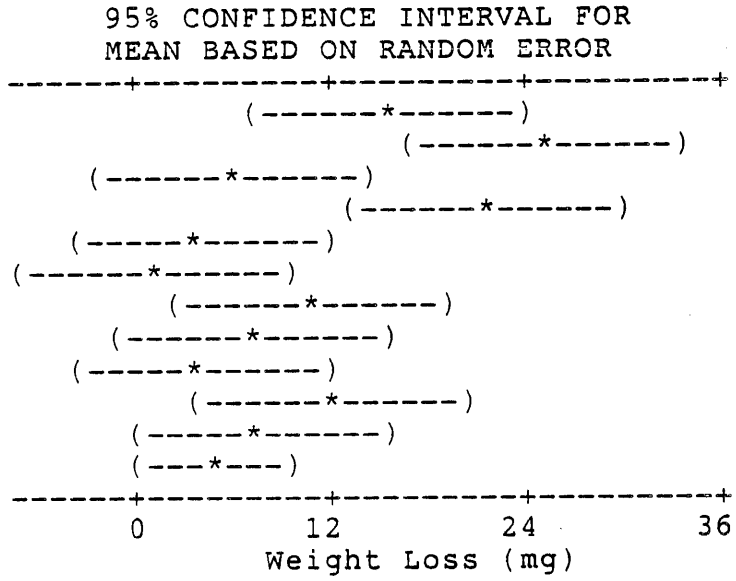

TABLE 3-8. ONE - WAY ANALYSIS OF VARIANCE OF WEIGHT LOSS FOR PAINT WITH CARBONATE EXTENDER.

ANALYSIS OF VARIANCE

SOURCE	DF	SS	MS	F	p
FACTOR	11	20216	1838	3.98	0.006
ERROR	16	7397	462		
TOTAL	27	27613			

EXPERIMENT	N	MEAN
SC 3	2	-1.20
SC 4	2	0.30
SC5	2	2.40
SC6	2	42.00
SC 9	2	-1.00
USC2	2	10.00
USC3	2	8.60
USC4	2	6.50
USC5	2	2.90
USC6	2	37.20
USC8	2	95.50
SC10,USC1,7	6	42.50

RANDOM ERROR = 21.50

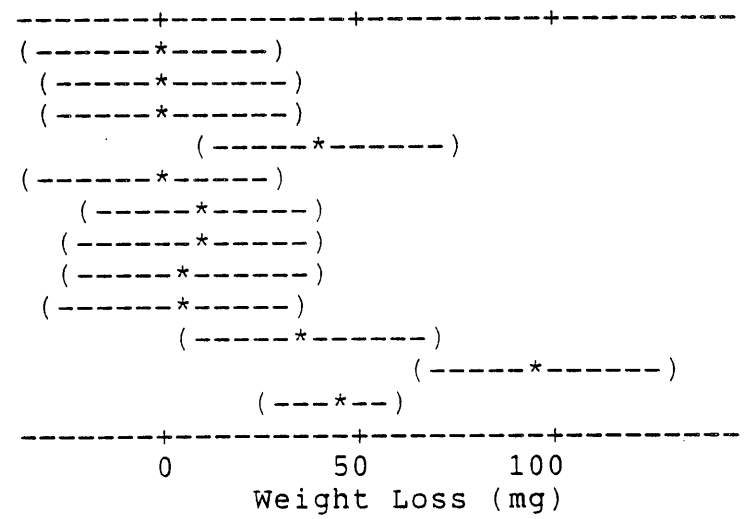

TABLE 3-9. ONE - WAY ANALYSIS OF VARIANCE OF WEIGHT LOSS FOR ALUMINUM.

ANALYSIS OF VARIANCE

SOURCE	DF	SS	MS	F	p
FACTOR	5	746.22	149.24	71.18	0.000
ERROR	6	12.58	2.10		
TOTAL	11	758.80			

EXPERIMENT	N	MEAN
USC3	2	0.400
USC4	2	1.200
USC5	2	2.900
USC6	2	22.800
USC7	2	0.900
USC8	2	4.300
RANDOM ERROR =		1.448

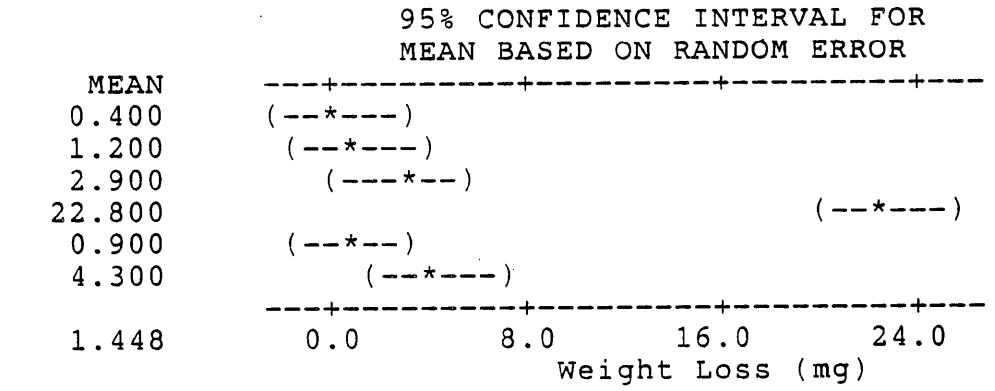

TABLE 3-10. ONE - WAY ANALYSIS OF VARIANCE OF STRENGTH LOSS FOR NYLON TEXTILE.

SOURCE	DF	SS	MS	F	p
FACTOR	6	456.35	76.06	12.07	0.001
ERROR	9	56.70	6.30		
TOTAL	15	513.06			

EXPERIMENT	N	MEAN
USC2	2	-2.000
USC3	2	-2.650
USC4	2	-1.850
USC5	2	5.700
USC6	2	14.700
USC8	2	3.550
USC1,7	4	1.425
RANDOM ERROR =		2.510

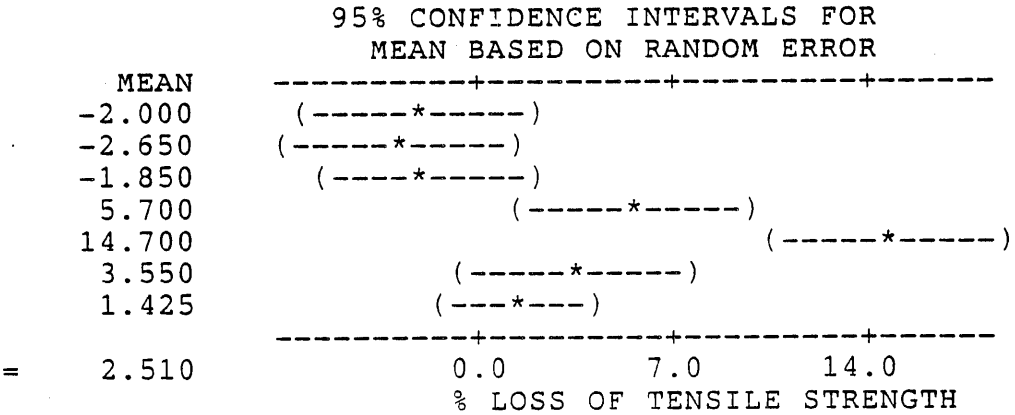

TABLE 3-11. SUMMARY OF THE STATISTICAL ANALYSIS OF THE LABORATORY DATA

X = 95% Statistically Significant Effect
O = No Statistically Significant Effect
\- = Material Not Used in Test
n.d. = No Data

CONDITIONS EXPERIMENT NO.	Zn	Ni	Low Carb. Paint	High Carb. Paint	Al	Nylon Fabric
BLANK USC2	O	O	O	O	n.d.	O
1 ppm Ozone SC3	O	O	X	O	-	-
0.5ppm Nitrogen Dioxide USC3	O	O	X	O	O	O
1 ppm Nitrogen Dioxide SC5	O	O	O	O	-	-
0.1 ppm Nitric Acid USC5	O	O	O	O	X	X
0.5 ppm Nitric Acid USC6	O	O	X	X	X	X
0.5 ppm Nitric Acid Low flow rate USC8	O	O	X	X	X	O
0.5 ppm Sulfur Dioxide USC4	X	X	O	O	O	O
1.0 ppm Sulfur Dioxide SC4	X	X	X	O	-	-
0.5 ppm each NO2,SO2 SC10, USC1, USC7	X	X	X	X	O*	X+
1.0 ppm each SO2,NO2 SC9	X	X	O	O	-	-
1 ppm each SO2,NO2,O3 SC6	X	O	X	X	-	-

* USC7 only,
\+ USC1, USC7 only.

any of the other materials; thus, lower levels of damage are measurable for this material than for the other materials studied. Paint free of carbonate extender showed small, but statistically significant, levels of damage due to O_3, NO_2, HNO_3, and SO_2. Also, the effects of NO_2 combined with SO_2 seem to be enhanced by the presence of O_3. A dosage effect for SO_2 significantly increased the damage to the paint.

Although the paint with carbonate extender showed more damage than paint without carbonate extender, there were fewer statistically significant effects because of the larger random errors for paint with carbonate extender, as seen in Table 3-8. Significant damage occurred in the presence of high HNO_3 concentration, SO_2 with NO_2, and SO_2, NO_2 and O_3 combined. No other statistically significant effects were observed.

Damage to aluminum is analyzed in Table 3-9. HNO_3 is responsible for all the significant effects. Damage due to HNO_3 increased with increasing concentration and decreased with lowered flow rate. This last result indicates that corrosion in the presence of HNO_3 was rapid and was limited by the availability of HNO_3.

The results of laboratory exposures of nylon textile are given in Table 3-10. As with aluminum, HNO_3 exposure resulted in significant damage and this damage increased with dosage.

3.2.3.2 Analysis of Corrosion Sensor Data

Two ACRMs each of zinc and of nickel were exposed in each laboratory experiment. As discussed in the report (9) which describes the design and testing of the ACRM, it was found that a zinc ACRM measures only about 10% of the total corrosion rate of a solid zinc panel exposed under the same condition. This is due to the effects of ohmic drop losses in the low conductivity electrolyte which covers the ACRM, current distribution and other factors which make the polarization resistance measurement principle (12) difficult to apply. The main

purpose of using the ACRM is to follow rapid changes in corrosion rates which are due to changes in the atmospheric conditions such as the cooling period of the laboratory tests or during episodes of acid rain and fog in the field tests. A formal statistical analysis of the ACRM data in Table 3-4 was not undertaken.

In general, there was little correlation between the integrated sensor response INT and weight loss for the same material obtained in the laboratory exposures. This is seen in Figure 3-21 which shows a plot of INT versus the weight loss for the galvanized steel coupons. Since corrosion rates were quite low, the sensor response was erratic in some cases with large differences in the signal for the two sensors of the same material.

There was a somewhat better correlation between the time of corrosion, t_{corr}, as determined by the ACRMs and the weight loss of galvanized steel as seen in Figure 3-22 for the zinc sensor.

The results for the nickel ACRM were similar, but showed even less correlation between weight loss and ACRM integration (INT) or t_{corr}.

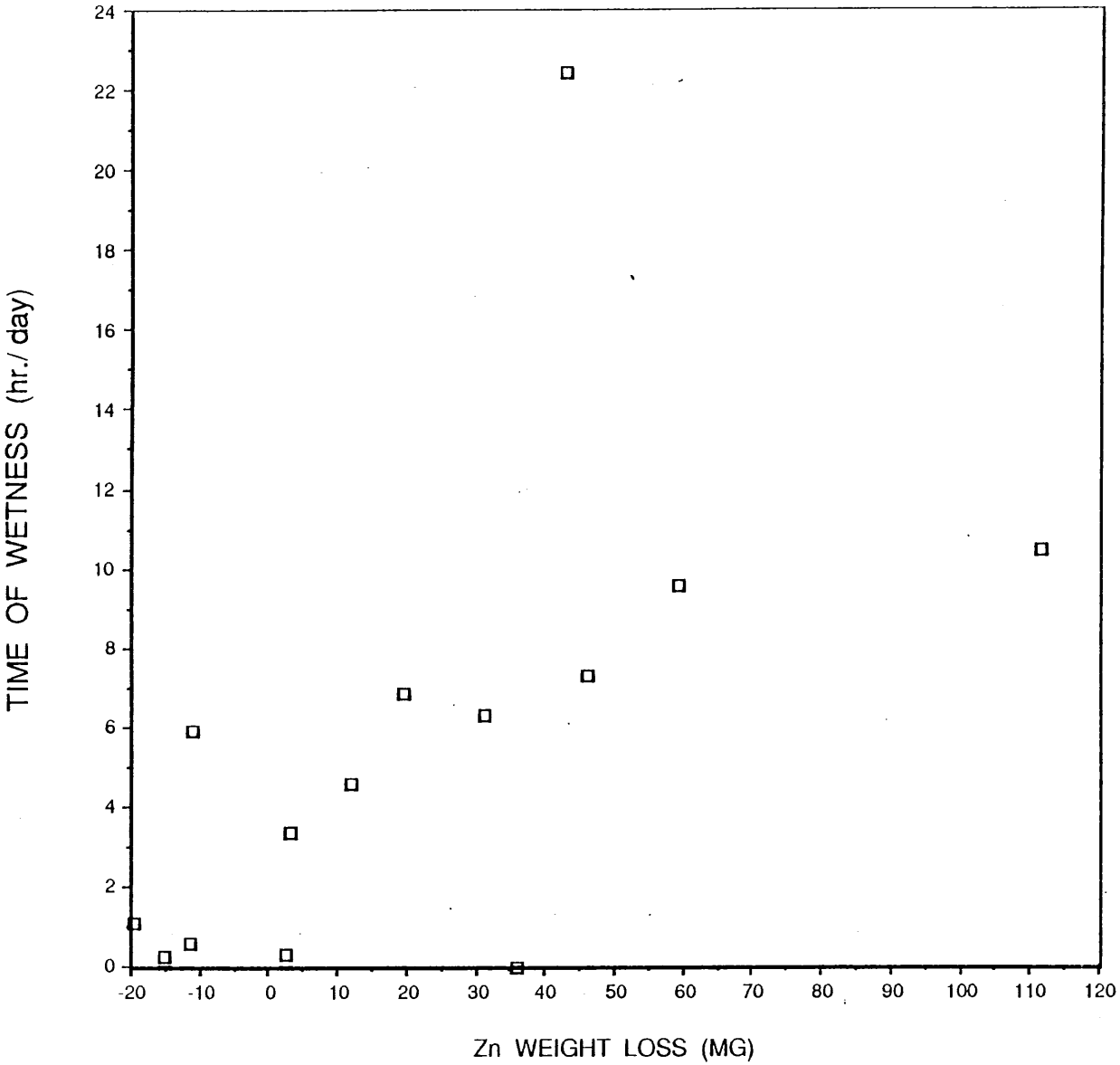

FIGURE 3-21. TIME OF WETNESS FOR ZINC SENSOR DATA VS. WEIGHT LOSS FOR GALVANIZED STEEL COUPONS.

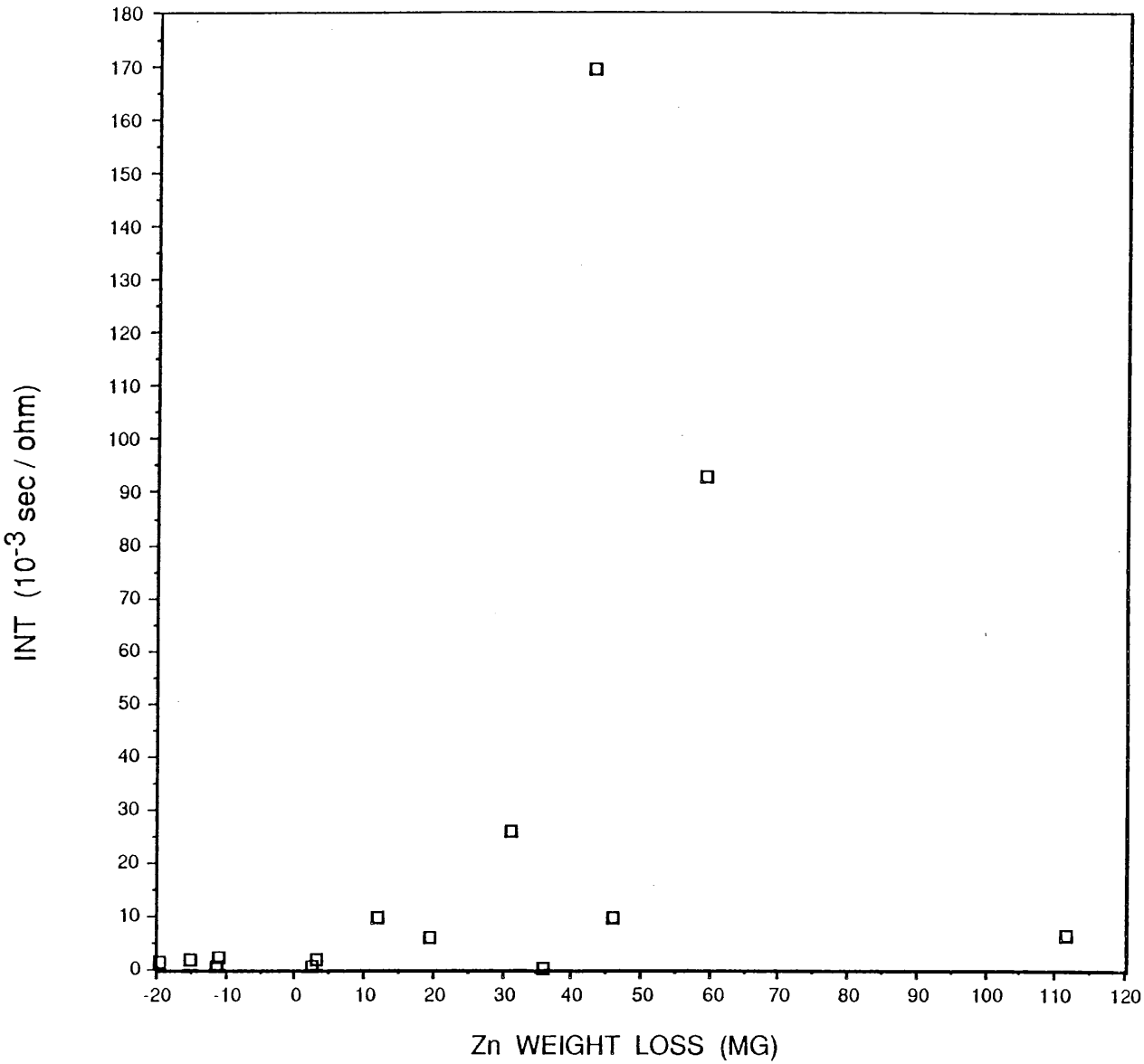

FIGURE 3-22. ACRM DETERMINATION OF ZINC SENSOR DATA VS. WEIGHT LOSS FOR GALVANIZED STEEL COUPONS.

4.0 DAMAGE FUNCTIONS

Damage functions were derived from weight loss and aerometric data at the four test sites, (Burbank, Long Beach, and Upland, and the background site in Salinas). More accurate formulae for interpolating current levels of damage in Southern California are given for previously listed materials, i.e., galvanized steel, nickel, paint without carbonate extender, and paint with some carbonate extender.

The development of damage functions relied on an analysis of the weight loss data described in Section 4.1 and on Atmospheric Corrosion Rate Monitor (ACRM) measurements described in Section 4.2 obtained in the field exposure tests. The latter were combined into daily averages and their relation to other aerometric variables investigated by Principal Component Analysis (PCA) (19). The PCA results were used to select the variables for inclusion into the damage functions.

4.1 ANALYSIS OF WEIGHT LOSS DATA

Figure 4-1 gives the approximate starting and ending time for the twelve exposure groups and Figures 4-2 to 4-5 give the average weight loss rates over each exposure period for each material at each site.

Two statistical tests of weight loss data were performed to determine differences between the sites: a standard one-way analysis of variance and a nonparametric paired sign test. Both tests gave the same results. For galvanized steel at Upland the weight loss rate was significantly lower than at the other three sites, which were not significantly different from each other. Ni had the greatest loss at Burbank and Long Beach followed by Upland and Salinas, where corrosion rates were significantly lower than at the Southern California sites.

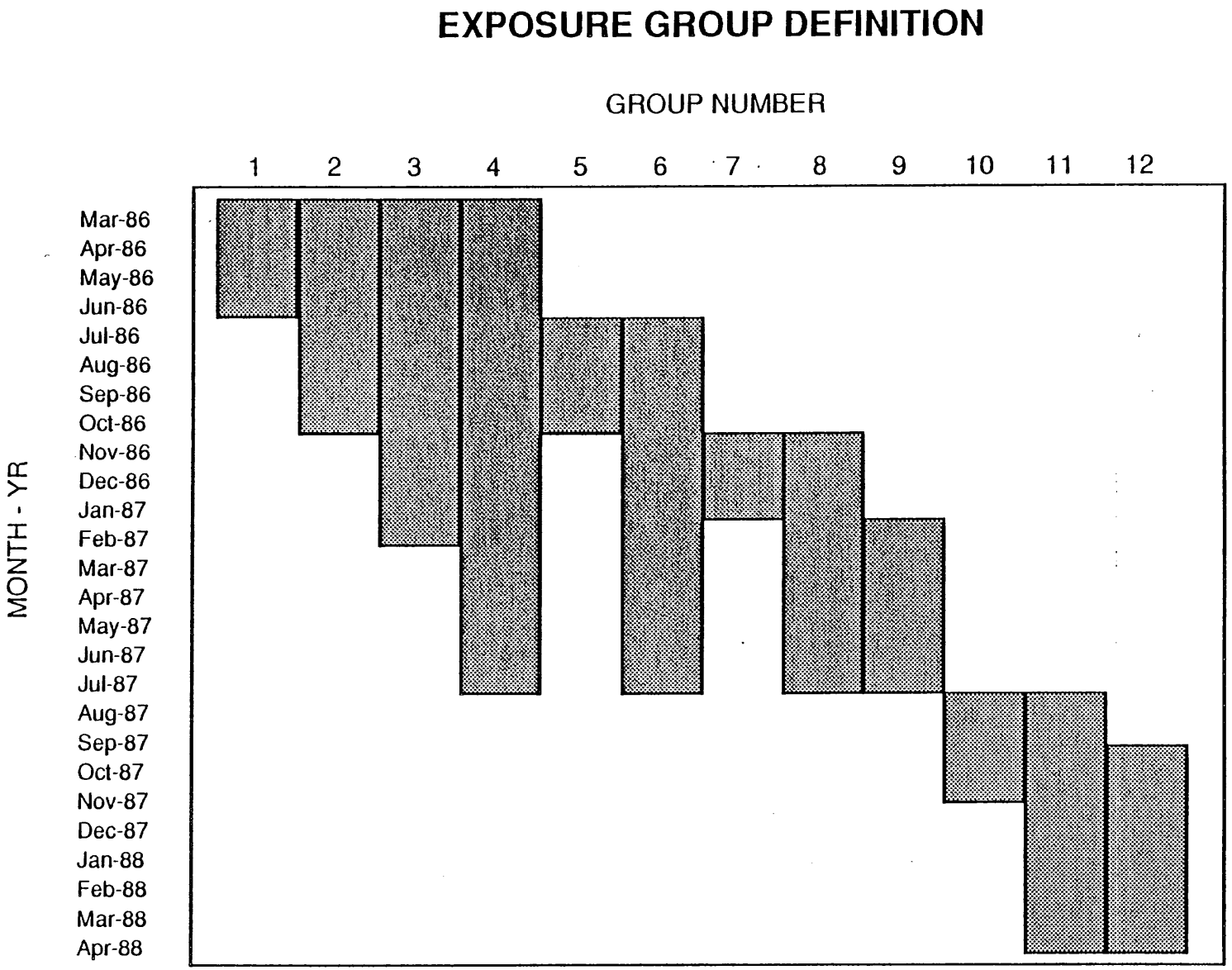

FIGURE 4-1. APPROXIMATE STARTING AND ENDING TIMES FOR THE TWELVE EXPOSURE GROUPS.

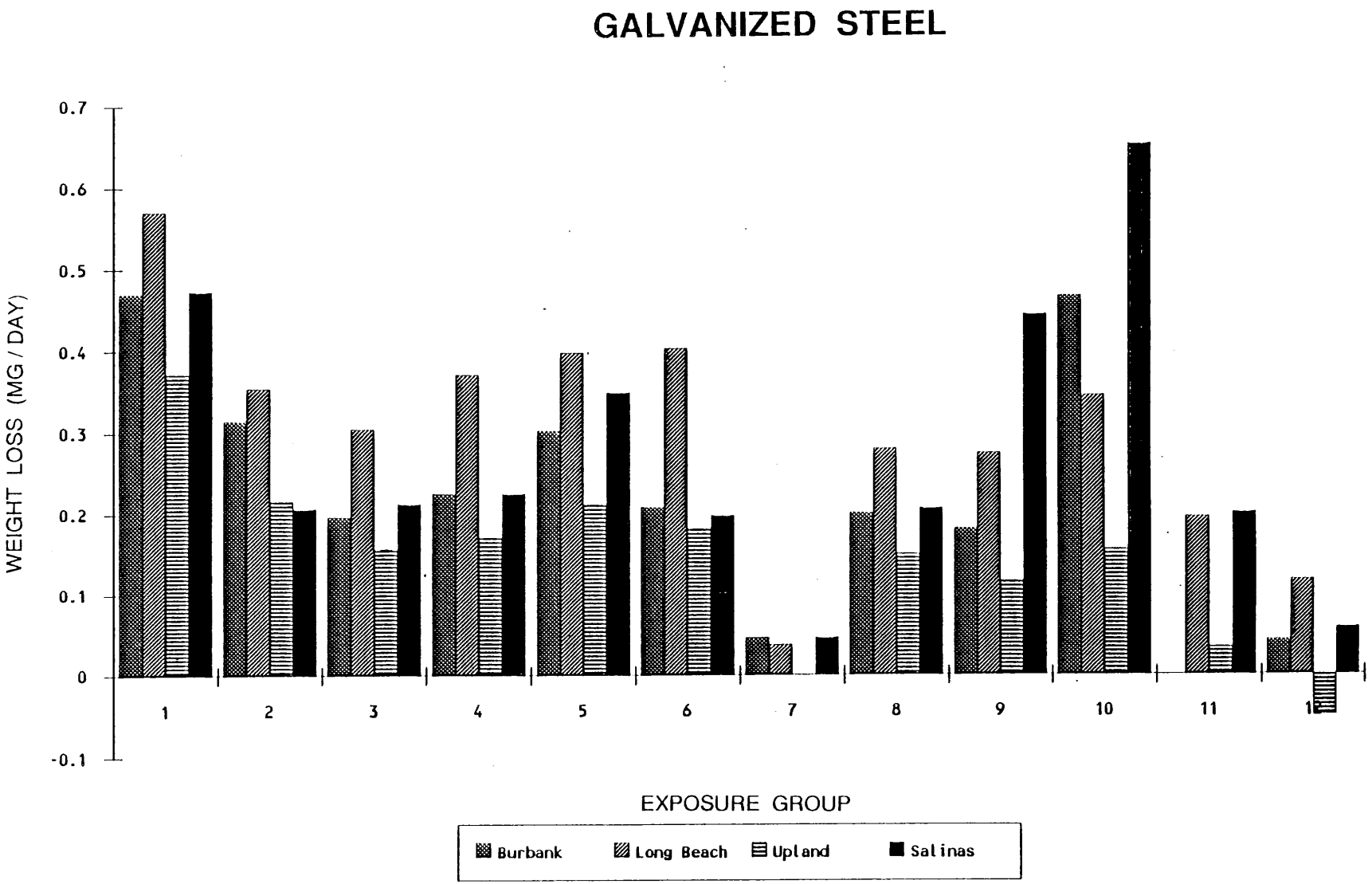

FIGURE 4-2. AVERAGE GALVANIZED STEEL WEIGHT LOSS RATES AT BURBANK, LONG BEACH, UPLAND, AND SALINAS SITES.

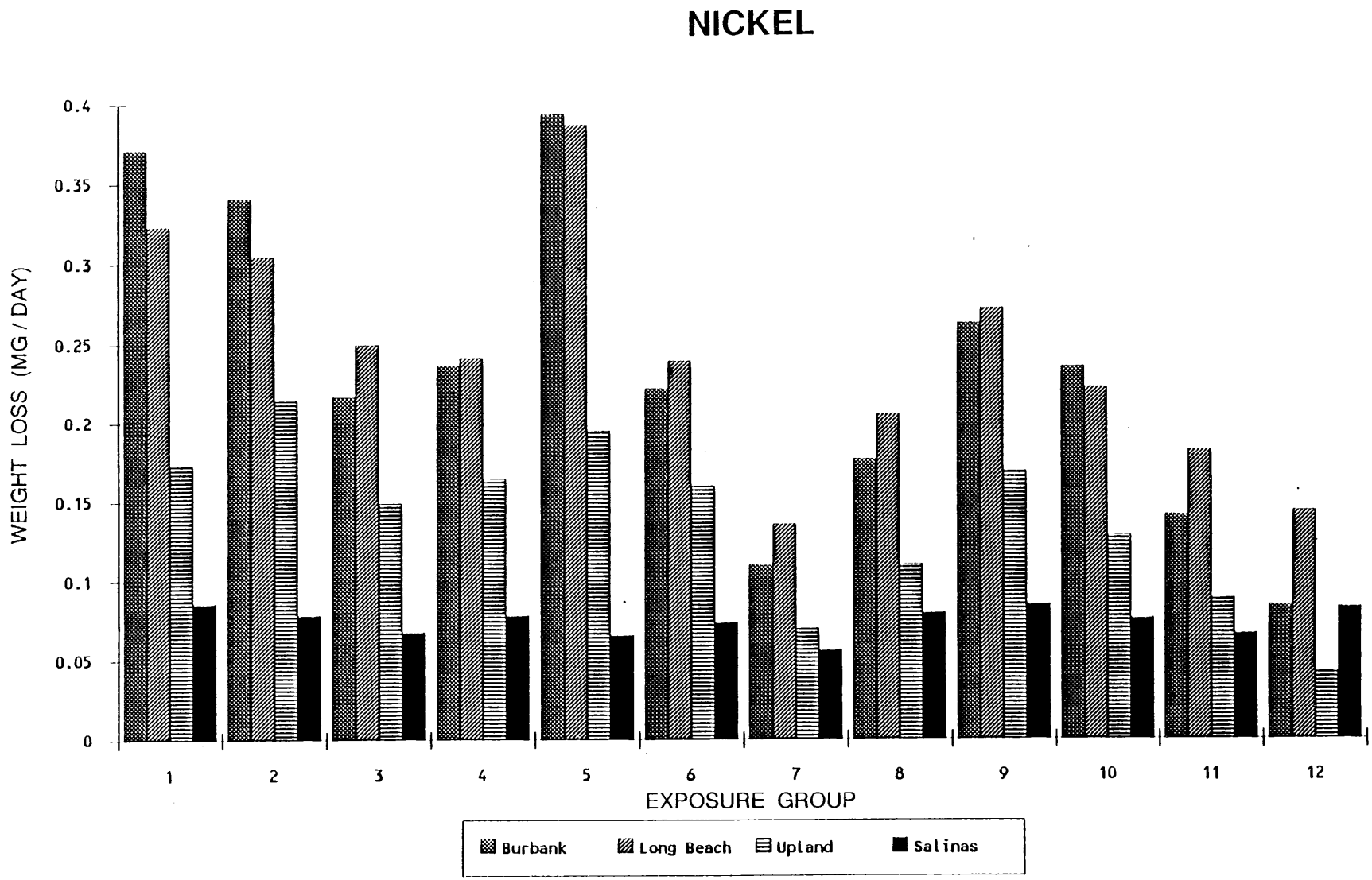

FIGURE 4-3. AVERAGE NICKEL WEIGHT LOSS RATES AT BURBANK, LONG BEACH, UPLAND, AND SALINAS SITES.

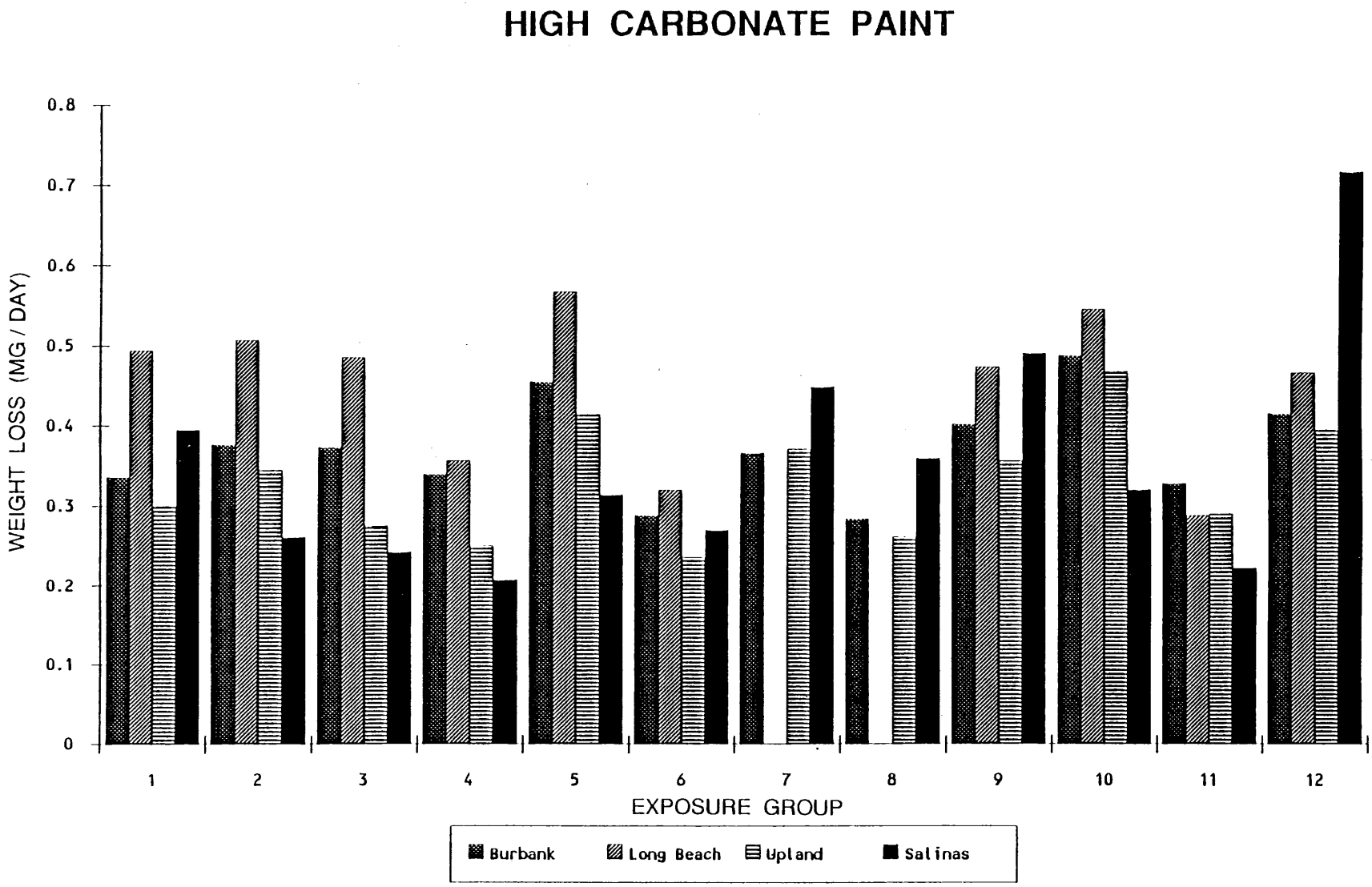

FIGURE 4-4. AVERAGE PAINT WITH CARBONATE EXTENDER WEIGHT LOSS RATES AT BURBANK, LONG BEACH, UPLAND, AND SALINAS SITES

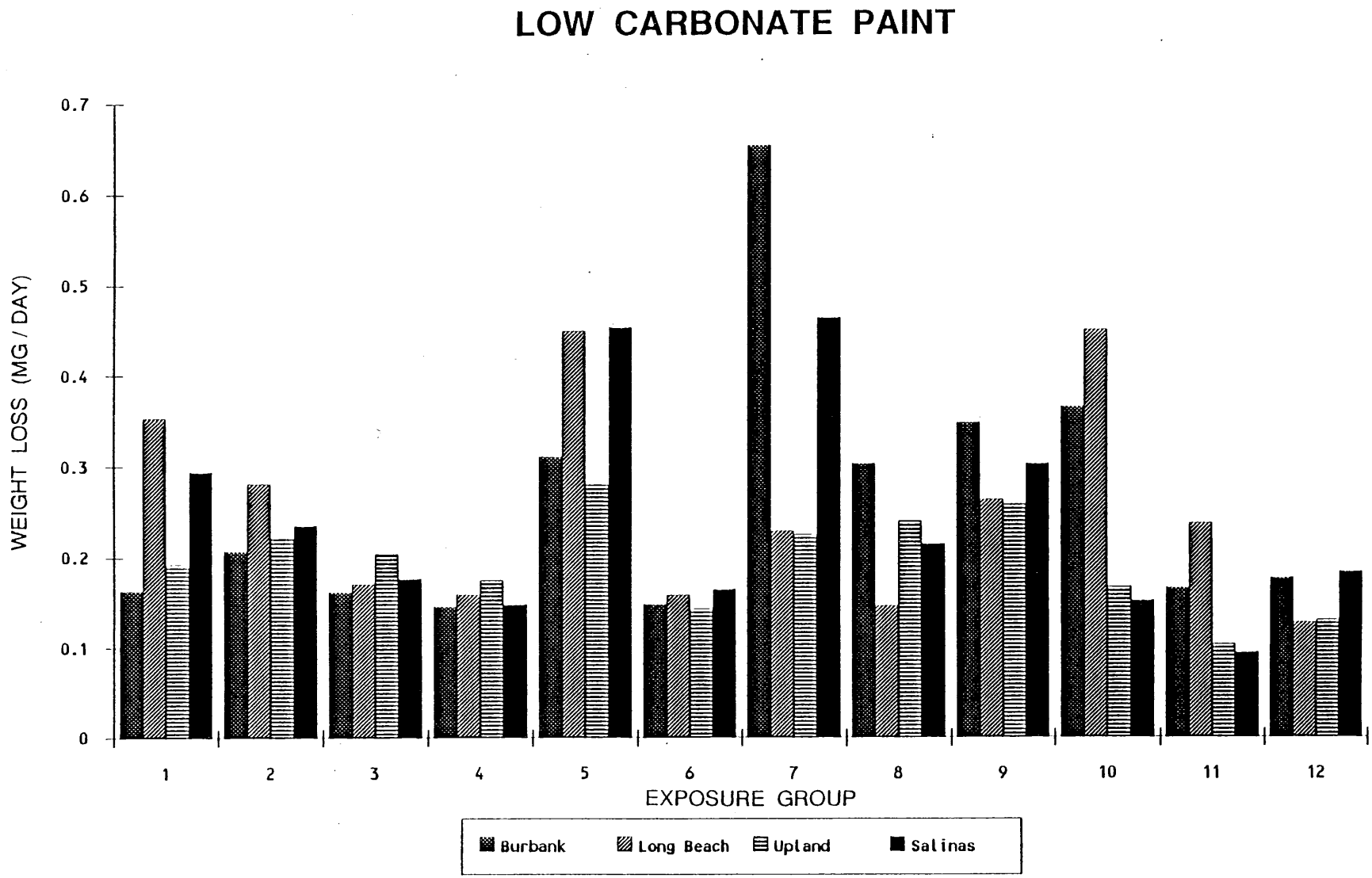

FIGURE 4-5. AVERAGE PAINT WITHOUT CARBONATE EXTENDER WEIGHT LOSS RATES AT BURBANK, LONG BEACH, UPLAND, AND SALINAS SITES

For paint with carbonate extender (high carbonate paint), the order of weight loss for sites in the L.A. Basin was Long Beach > Burbank > Upland; however, damage at Salinas was not significantly lower than at the L.A. sites. The low carbonate paint (extender-free) showed no significant differences between any of the sites. This lack of significant differences between sites for low carbonate paint makes it unlikely that a damage function for this material can be found.

4.2 ANALYSIS OF ACRM DATA

The goals of the ACRM data analysis were: 1) comparison of ACRM averages (integrated corrosion loss INT (Section 3.1.3)) and observed weight loss data, 2) a general statistical description of the data, and 3) a determination of the relationship of ACRM data to air quality and meteorological data. The results of this analysis provided insight into the atmospheric corrosion processes in California and guided the selection of variables to be included in the damage functions.

4.2.1 Comparison of Observed Weight Loss Rates and ACRM Data

Average weight loss rates for each site and material were determined by dividing the weight loss by the number of days the material was exposed. Actual exposure times were used in the calculation, not average or intended exposure times. The average ACRM data for the zinc (Zn) up, Zn down, nickel (Ni) up, and Ni down sensors for each exposure period were also calculated. The correlations of the sensor and weight loss data for all sites and materials were calculated. It was found that the Ni up sensor data correlated well with observed Ni weight loss at all sites, as shown in Figure 4-6. The relationship between sensor data and weight loss was nearly the same at Burbank and at Long Beach. At Upland there seemed to be a different relationship, while the Salinas data had too little variation to draw reliable conclusions. Also, the Salinas data had too much missing data for the values to be a good estimate of the average sensor values for the exposure periods.

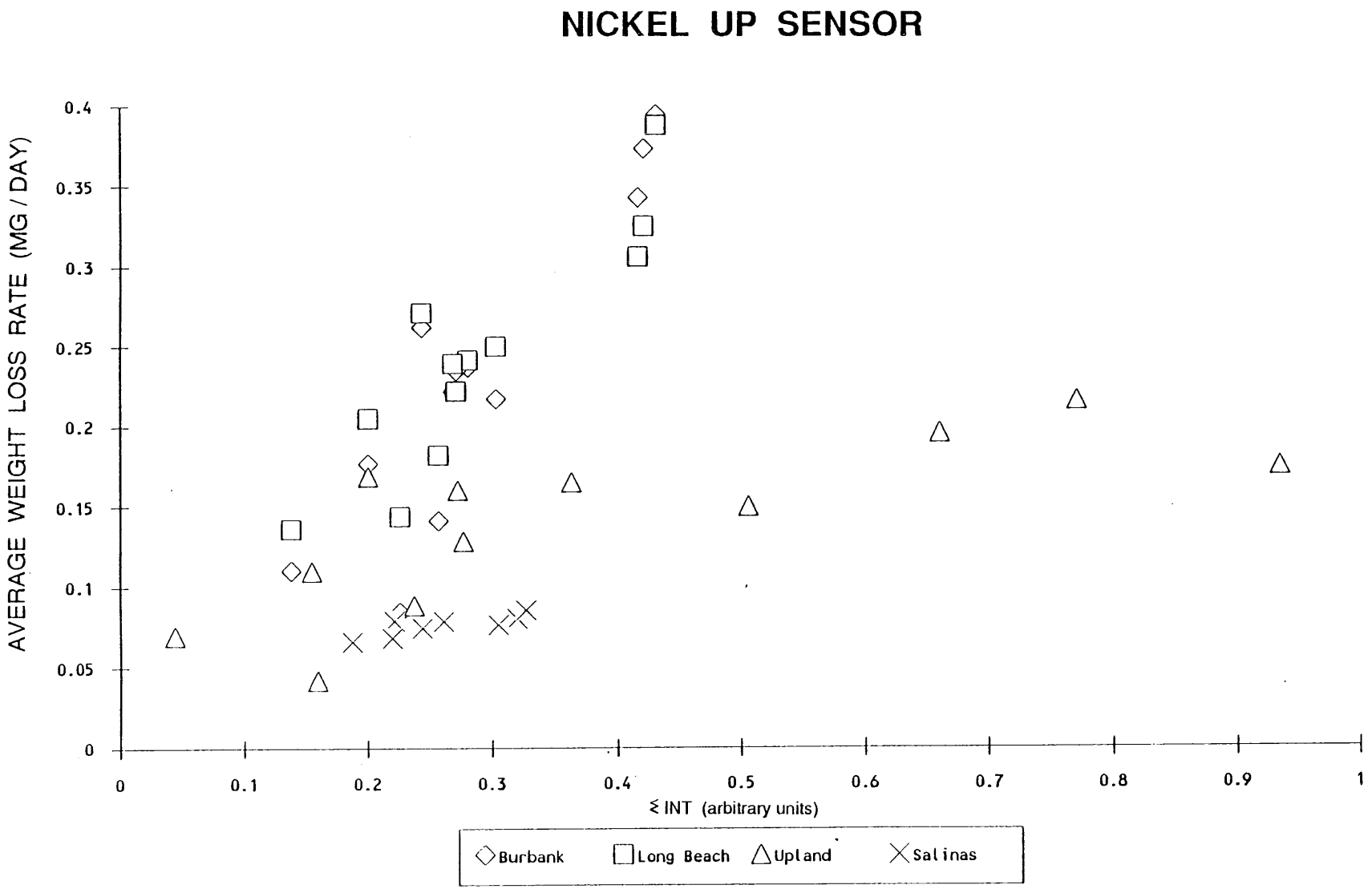

FIGURE 4-6. AVERAGE WEIGHT LOSS RATE VS. ACRM NICKEL UP SENSOR DATA.

At this point it has to be remembered that the weight loss data are the average weight loss for both sides of a panel, while the ACRMS provide corrosion rate data for the sensor facing the sky ("up") and the sensor facing the ground ("down"). Considering the short exposure times and the low corrosion rates, it is possible that the weight loss for each side of a panel was quite different. In this case difficulties could arise in correlation between the separate "sensor up" and "sensor down" data and the average weight loss for the panel. Different corrosion rates and different time dependence of corrosion rates have been observed for skyward and groundward surface of Al alloys (21).

The Ni up sensor data also correlated well with the observed Zn damage and slightly less with the high carbonate paint damage, but it did not correlate with the low carbonate paint weight loss. None of the INT data for the other three sensors consistently correlated well with any of the weight loss data. Statistical analysis was restricted to the Ni up sensor because it the was the only one related to observed damage. Sensor data from Salinas were judged to be unreliable because of long periods of missing data; thus, only the Ni up ACRM data from the three Southern California sites were subjected to further statistical analysis.

4.2.2 Seasonal Variations of the ACRM Data

The plot of cumulative Ni up sensor data versus time at Long Beach (Figure 4-7) shows that damage is very low during the Southern California winter season, October to April. This at first seems somewhat paradoxical since moisture and primary pollutant concentrations are high during the winter months. Virtually all the observed corrosion damage occurs during the smog season, April to September. Very similar results have been obtained for the weight loss data (3.1.1). This result suggests that corrosion in Southern California is primarily associated with pollutants and conditions found with photochemical smog. A more detailed analysis of the ACRM data in Southern California follows.

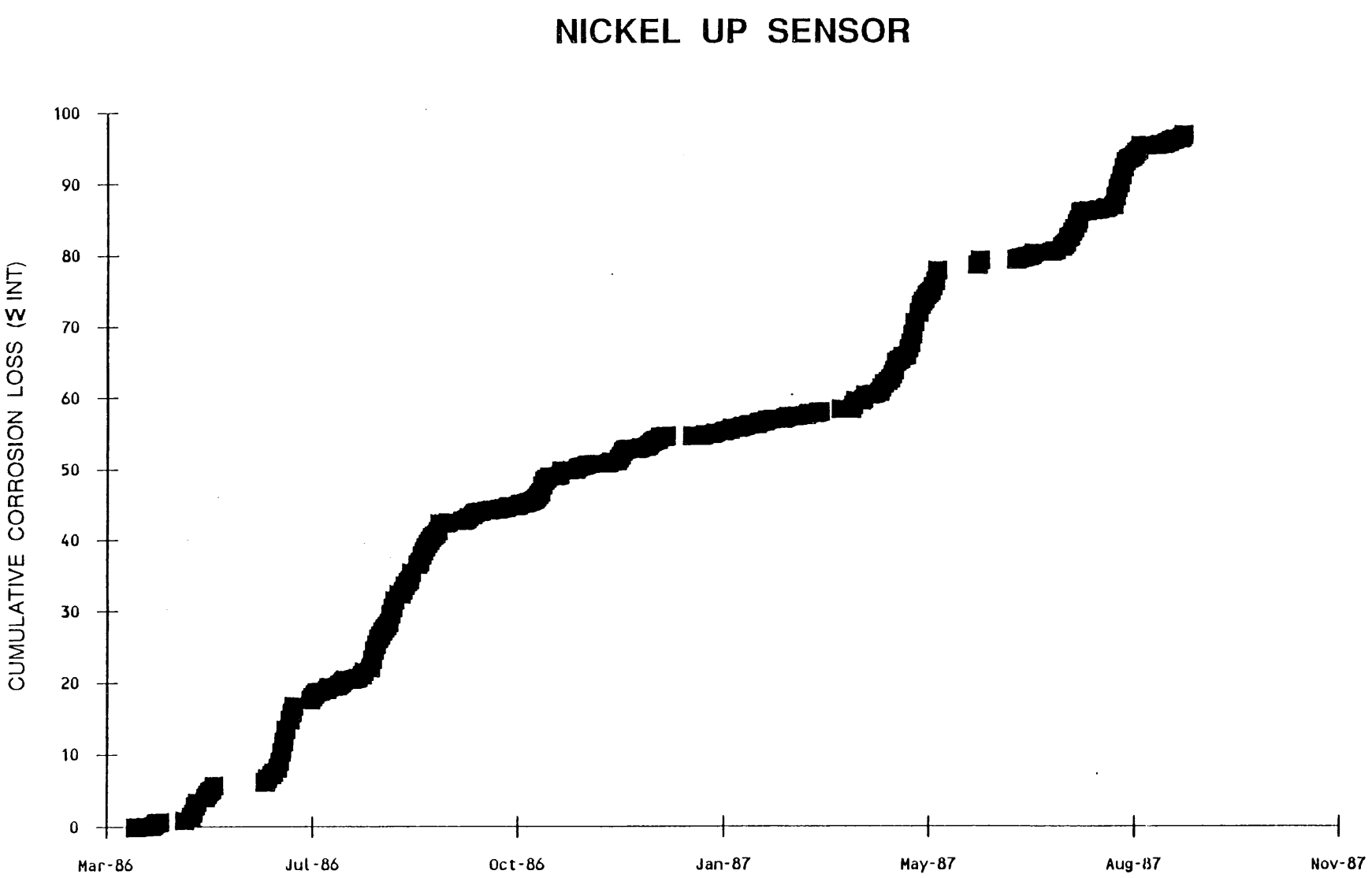

FIGURE 4-7. CUMULATIVE CORROSION LOSS FOR NICKEL UP SENSOR DATA AT LONG BEACH.

4.2.3 Relationship of ACRM Data with Air Quality and Meteorological Variables

An important part of the study design was the colocation of the exposed materials with air quality monitoring sites. The Air Resources Board provided hourly air quality and meteorological data for the four sites for the period January, 1986, to January, 1988. Additional data extending to April, 1988, for the Southern California sites were obtained directly from the South Coast Air Quality Management District.

All the data were reduced to daily averages and calculated on a midnight to midnight basis. Daily averaging was used for several reasons. First, the variation in the ACRM data, humidity, temperature, and the pollutant gas concentrations is dominated by the diurnal cycle in emissions, mixing heights, wind speed, and temperature. Averaging over 24 hours removes these cycles and highlights the underlying relationships in the data. Second, the particulate data are 24-hour averages. A list of variables included in the analysis is given in Table 4-1.

At least three data sets were constructed for each site. One consisted of the corrosion loss determined with the ACRM, air quality and meteorological variables; a second added time-of-wetness variables; and the third included all the variables in the first two sets plus airborne particulate mass and composition data. These data sets were analyzed by Principal Component Analysis (PCA), a multivariate statistical technique which is capable of determining the basic underlying physical processes influencing the data; see Henry and Hidy (19) for a discussion of the interpretation of PCA of air quality data.

A typical PCA result is given in Table 4-2. Of the twelve variables in this particular analysis, 92% of the variability can be explained by only 5 statistically independent Principal Components (PC). The first PC is the single linear combination of the variables best explaining the

TABLE 4-1. VARIABLES USED IN ANALYSIS OF ACRM DATA

1. Air quality variables

   CO, SO_2, NO, NO_2, O_3 - Daily averages and daily 1 hr. maximum
   TSP, PM-10, sulfate and nitrate daily ave. every sixth day

2. Meteorological variables

   Rack t - Temperature on exposure rack
   Rh - Relative humidity measured on the exposure rack
   T40 - Fraction of time Rh < 40%
   T60 - Fraction of time Rh < 60%
   T80 - Fraction of time Rh < 80%
   Wind speed - measured at monitoring site
   Rain - Rainfall amount at L.A. City Hall

TABLE 4-2. PRINCIPAL COMPONENT ANALYSIS OF BURBANK AIR QUALITY AND METEOROLOGICAL DATA.

Variable	Principal Component 1	2	3	4	5
CO AVG	0.957	0.099	0.178	-0.013	-0.154
SO_2 AVG	0.708	-0.015	0.307	0.103	0.579
NO AVG	0.953	0.087	-0.108	-0.063	-0.173
NOx AVG	0.974	0.032	0.076	-0.011	-0.180
O_3 AVG	-0.479	-0.430	0.634	0.098	-0.032
NO_2 AVG	0.614	-0.167	0.676	0.175	-0.128
Rack t	-0.683	-0.401	0.420	0.172	-0.047
RH	-0.218	0.918	0.232	-0.095	-0.030
T40	-0.336	0.834	0.264	-0.143	-0.108
T60	-0.231	0.895	0.237	-0.098	-0.084
T80	0.156	0.848	0.000	0.105	0.270
RAIN	-0.047	0.409	-0.237	0.868	-0.110
Eigenvalue	4.5816	3.6126	1.4159	0.8874	0.5461
Proportion	0.382	0.301	0.118	0.074	0.046
Cumulative	0.382	0.683	0.801	0.875	0.920
Interpretation	High primary pollutants in winter	High Rel. Hum.	Photochem. smog	Rain	Sulfur dioxide
Correlation with Ni up sensor	-0.359	0.051	0.298	0.018	0.035

overall variation. In this case the first PC explains 38% of the variability in the 12 variables in the analysis. The variables which contribute most strongly to this PC are the primary pollutant gas concentrations, and temperature which contributes negatively; i.e., when the primary pollutant gases are high it is low and vice versa. This component can be interpreted as representing cold, stagnant winter conditions that bring high concentrations of primary pollutants.

The second PC is the linear combination of the variables, statistically independent of the first PC, that explains a maximum of the variability not covered by the first PC. In this case, 30% of the variability in the data set is associated with humidity related variables (RH, T40, T60, T80). The third PC explains 12% of the data variability and, like all the PCs, it is statistically independent. Being most strongly correlated with O_3, NO_2, and temperature, this component can reasonably be associated with photochemical smog intensity. Finally, the minor fourth and fifth components explain only 7% and 5% of the data, respectively, with the fourth PC strongly associated with the occurrence, rare in Los Angeles, of rain. The fifth component almost solely depends on SO_2 concentration. Clearly, the PCA of the Burbank data uncovered five basic air quality and meteorological conditions: high primary pollutants, high humidity, photochemical smog, rain, and high SO_2 concentrations. Since the PCs are independent, these conditions also occur independently of each other.

The relationship of the ACRM corrosion rate data to these basic meteorological and air quality conditions was investigated by correlation analysis and also by performing a multiple linear regression of the daily averaged ACRM data on the values of the PCs. Data from all sensors were analyzed, but since Ni up was the only sensor clearly related to observed damage, only those sensor results are discussed here. The final row of Table 4-2 gives the correlation of the Ni up sensor with the five PCs. There is a moderately negative correlation with the first PC, indicating that corrosion is low during the winter months even though acidic gas concentrations are high. This agrees with

the pattern of seasonal variation in weight loss data noted above (see also Figure 4-7). Corrosion damage has a moderately positive correlation with the photochemistry component and no correlation with the other PC's. The failure to see any relationship of corrosion to SO_2 levels is noteworthy; however, even at Long Beach, which has the highest SO_2 concentration, the annual average is less than 10 ppb (Table 2-3). The lack of dependance of corrosion rates determined from the sensors on humidity variables suggests that the observed seasonal variations of corrosion rates are due to variations in pollutant levels.

Regression of the Ni up sensor data on the PCs was similar to the correlation results discussed above. For example, the Ni up sensor at Burbank was not strongly related to any of the principal components. Only 22% of the sensor variability could be explained by the regression, with the first and third PCs accounting for almost all of this. The regression shown corrosion, as measured by the Ni up sensor, is high when the primary pollutants are low and photochemistry is high. Apparently SO_2 levels in Los Angeles are so low, even in the winter, that a strong effect cannot be observed. In fact, it seems that an inhibiting effect, such as washing and cleaning by rain, occurs in the winter.

The results of similar PCA and regression analysis of the data from other sites in Long Beach and Upland followed the same general pattern: negative dependence of corrosion rates on primary pollutants, high corrosion with high photochemical smog, and little or no dependence on the humidity related PC. There were some variations in these basic results, with Long Beach having a much stronger SO_2 component than the other sites, presumably because of the proximity of major sources of this pollutant. Similarly, the photochemical component in the Upland data was stronger than at the other sites, being consistent with the known dominance of photochemical smog at sites in the eastern Los Angeles basin.

4.2.4 Summary of ACRM Analysis Results

1. Corrosion rates have a maximum in the summer and fall and a minimum in the spring and winter.

2. The corrosion loss determined with the Ni-up sensor correlates very well with observed Ni weight loss rates, quite well with zinc weight loss rates, somewhat with high carbonate paint loss, and poorly with low carbonate paint loss. The latter result is not surprising since the weight loss for the low carbonate paint was not site dependent.

3. Principal component analysis of the sensor data with other aerometric variables indicates that corrosion is correlated with periods of high photochemical smog. Corrosion is negatively correlated with periods of high primary pollutants (SO_2, NO_2, CO). There is little or no dependence on an independent high relative humidity factor.

4. Based on the PCA, correlation and graphical analysis, O_3, NO_2, T60, and their cross products were selected for development of damage functions. T60 is the fraction of time during the day when the relative humidity exceeds 60 per cent.

4.3 DAMAGE FUNCTIONS FOR GALVANIZED STEEL, ALUMINUM, AND PAINT WITH CARBONATE EXTENDER

Damage functions were determined by regression of weight loss rates (weight loss divided by number of exposure days) against the explanatory variables, in this case O_3, NO_2, T60, O_3 x T60, NO_2 x T60, and O_3 x NO_2 averaged over the exposure period. Other sets of variables were considered, but either performed poorly or were not physically reasonable. O_3 and NO_2 do not themselves cause damage, they are

surrogates for the components of photochemical smog that presumably cause damage, such as HNO_3 vapor, organic acid, and acidic particles.

The damage functions are of the form:

$$L = \sum_{1} a_i V_1$$

where the explanatory variables, V_i, are either average gas concentrations or humidity related variables. The humidity related variables, such as T60, are numbers from zero to one, and the weight loss rate, L, is in grams/m^2/yr.

Determination of the damage functions was hampered by insufficient data. Exposure groups 11 and 12 (Figure 4-1) at all the Southern California sites could not be used due to a lack of relative humidity data in 1988. The operation of the ACRMs and the RH - temperature probe at Burbank and Long Beach was stopped in January 1988. Group 10 at Burbank was eliminated for the same reason, leaving a set of twenty-nine points for the Southern California sites. For Salinas, all of the groups had too little valid data, either aerometric or humidity, to allow analysis, this presents a serious problem, since Salinas is the background site, the only low pollution site in the data set. This exclusion makes it impossible to determine a damage function that can be used to estimate damage at low or zero pollution levels. For this reason two sets of damage functions were calculated. One was determined from the Southern California data alone and can be used only to interpolate current damage levels in Southern California, and one that can be used to estimate damage at all locations for all pollution levels.

This second set of damage functions was determined by adding a single point to the Southern California data set that consists of average values of the variables in Salinas. These damage functions are less certain than the other set, but they can be applied to estimate

damage at low pollution levels.

The coefficients and associated errors of the two sets of damage functions are given in Tables 4-3 and 4-4. Note that these functions are only valid for estimating seasonal or yearly average damage, and that the input gas concentrations are daily averages for a season or a year. Application to shorter time periods will lead to absurd results. Similarly, application of the formula in Table 4-3 to pollution levels lower than those currently found in Southern California will yield inaccurate or even negative results.

4.4 OTHER DAMAGE FUNCTIONS FOR OTHER VARIABLES

For low carbonate paint (extender free) weight loss, a statistically significant damage function could not be determined. As discussed in 3.1.1.3, corrosion damage was not site dependent.

Damage functions for aluminum, nylon fabric, and painted wood were not determined at this time because of insufficient damage and aerometric data.

TABLE 4-3. COEFFICIENTS FOR DAMAGE FUNCTIONS FOR CURRENT POLLUTION LEVELS AT SOUTHERN CALIFORNIA SITES.

	Zinc	Nickel	Hi. Paint
Constant	10.41	8.79	-5.716
error	2.98	2.24	2.465
O_3 Coeff.	-0.3408	-0.3305	-
O_3 error	.1025	0.0770	
NO_2 Coeff.	-0.1536	-0.1244	0.1494
NO_2 error	0.0519	0.0389	0.0486
T_60 Coeff.	-	-	19.14
T_60 error			4.89
O_3 x T60 Coeff.	0.1874	0.1184	-
O_3 x T60 error	0.0496	0.0372	
NO_2 x T60 Coeff.	-	-	-0.3284
NO_2 x T60 error			0.1034
O_3 x NO_2 Coeff.	0.004641	0.00507	-
O_3 x NO_2 error	0.001728	0.00130	
Standard Error of Estimate	0.768	0.576	0.579
R-squared	0.560	0.518	0.572

TABLE 4-4. COEFFICIENTS FOR DAMAGE FUNCTIONS FOR ALL POLLUTION LEVELS AT ALL CALIFORNIA SITES.

	Zinc	Nickel	Hi. Paint
Constant	-1.174	-0.118	-.031
error	1.051	0.7360	1.120
O_3 Coeff.	0.0326	-0.0572	-
O_3 error	0.0199	0.0287	
NO_2 Coeff.	-	-	0.03324
NO_2 error	-		0.01681
T60 Coeff.	5.252	3.307	3.98
error	1.457	1.053	1.09
O_3 x NO_2 Coeff.	-	0.00154	-
O_3 x NO_2 error	-	0.000534	
Standard Error of Estimate	0.998	0.6744	0.708
R-squared	0.326	0.354	0.351

5.0 REFERENCES

1. Salmon, R.L. "Systems Analysis of the Effects of Air Pollution on Materials." APTD-0943, U.S. Department of Health, Education and Welfare, National Air Pollution Control Administration, Raleigh, North Carolina, 1970.

2. Yocom, J.E. and N.S. Baer. "The Acidic Deposition Phenomena and Its Effects - Critical Assessment Review Papers." Volume III, Public Review Draft, EPA-600/8-83-016B, 1983.

3. Topol, L. and R. Vijayakumar. "Materials Damage Functions of Acidic Air Pollutants: A Literature Review." Draft Report, EPRI Contract No. RP2071, 1983.

4. Spence, J., and F. Haynie. Final Report on the EPA Workshop on Acid Deposition on Painted Surfaces. EPA, Research Triangle Park, NC, 1985.

5. Mansfeld, F. Amer. Society for Testing & Materials SOP 727, 215, 1981.

6. Mansfeld, F., "New Approaches to Atmospheric Corrosion Research Using Electrochemical Techniques." Corrosion Processes, Appl. Science Publ.

7. Mansfeld, F., S.L. Jeanjaquet, M.W. Kendig and D.K. Roe, Atmosph. Envir. 20, 1179, 1986.

8. Mansfeld, F., Electrochem. Soc., 135, 1354, 1988.

9. Mansfeld, F. "Development and Evaluation of an Instantaneous Atmospheric Corrosion Rate Monitor." Final Report, EPA, Contract No. 68-02-3731, 1984.

10. Mansfeld, F., and R. Vijayakumar, Corr. Sci. 28, 939, 1988.

11. Mansfeld, F., and R. Vijayakumar, 81st APCA Meeting, paper No. 1514, June 1988.

12. Mansfeld, F. "The Polarization Resistance Technique for Measuring Corrosion Rates." in Adv. Corr. Sci. and Techn., Plenum Press, Vol. 6, p. 163, 1976.

13. Hess's Paint Film Defects. Edited by H.R. Hamburg and W.M. Morgans, 3rd Ed., Chapman Hall, 1979.

14. Johnston-Feller, R. and D. Osmer; "Exposure Evaluation: Quantification of Changes in Appearance of Pigmented Materials", J. Coating Tech., 49, 25-36, 1977.

15. Mansfeld. F., R. Henry, and R. Vijayakumar. "The Effects of Acid Fog and Dew on Materials, Final Report, CARB, Contract No. AS-138-32.

16. Solomon, P., California Institute of Technology, Personal Communication, 1985.

17. Mansfeld F., and S.L. Jeanjaquet. "Investigation of the Effects of Acid Deposition on Materials", Final Report SC5450.FR, Rockwell Inst. Test Center, Sept. 1987.

18. Kucera, V., and E. Mattson. "Atmospheric Corrosion", in "Corrosion Mechanisms", F. Mansfeld, editor, M. Dekker, 1987.

19. Henry, R.C. and G.M. Hidy. "Multivariate Analysis of Particulate Sulfate and Other Air Quality Variables By Principal Components, Part 1 Annual Data from Los Angeles and New York". Atmospheric Environment, Vol 13, pp 1581-1596.

20. Legault, R.A. and V.P. Pearson. Amer. Society for Testing & Materials STP 646, 83, 1978.

List of Inventions Reported and Publications

The following publications were a result of this program:

Manfeld, F., and R. Vijayakumar, 81st APCA Meeting, paper No. 1514, June 1988.

Vijayakumar, R., and F. Mansfeld, "Materials Damage Due to Acid Deposition - A Field Study in Southern California," Corrosion 187, NACE, paper No. 413, San Francisco, CA, March 1987.

Mansfeld, F., and R. Vijayakumar, Corr. Sci. 28, 939 (1988).

No patents resulted from this program.

GLOSSARY OF TERMS, ABBREVIATIONS AND SYMBOLS

CARB	California Air Resources Board
EMSI	Combustion Engineering Environmental's Environmental Monitoring and Services
RISC or SC	Rockwell International Science Center
USC	University of Southern California
CEEL/USC	Corrosion and Environmental Effects Laboratory/ University of Southern California
RH	Relative Humidity
ACRM	Atmospheric Corrosion Rate Monitor
ACRMDL	Atmospheric Corrosion Rate Monitor Data Logger
ACM	Atmospheric Corrosion Monitor
T60	Percentage of Time that RH >60%
T70	Percentage of Time that RH >70%
T80	Percentage of Time that RH >80%
PC	Principal Component
PCA	Principal Components Analysis
NAPAP	National Acid Precipitation Assessment Program
ISO	International Standards Organization
tw	Time-of-Wetness
Rp	Polarization Resistance
i_{corr}	Corrosion Time
B	Theoretical value B = 20 mV
ATEC	Atmospheric Technology, Inc.
INT	Corrosion Loss for a 12 hr time period (Integrated)
t_{corr}	Corrosion Time
SCAB	South Coast Air Basin
Al Vi	) Variables in Damage Function)

APPENDIX - METHODOLOGIES

APPENDIX - METHODOLOGIES

Table of Contents

		Page
1.0	MATERIAL SAMPLE PREPARATION, COMMON METHODOLOGIES	114
1.1	PREPARATION OF MATERIALS, MATERIAL SPECIFIC	117
	Nickel	117
	Galvanized Steel	117
	Paint on Stainless Steel	118
	Paint on Wood	119
	Nylon Fabric	120
	Aluminum	121
	Polyethylene	122
	Concrete	123
1.2	DAMAGE MEASUREMENT OF MATERIALS	124
1.2.1	Weight Loss Group	124
	Nickel	125
	Galvanized Steel	126
	Aluminum	127
	Paint on Stainless Steel	128
	Concrete	129
	Strength Loss for Nylon Textile	130
1.2.2	Appearance Measurement	131
1.2.3	Polyethylene Damage Measurements	131
1.3	FIELD EXPOSURE RACKS	131
1.4	LABORATORY TESTS	132
1.5	ATMOSPHERIC CORROSION RATE MONITOR (ACRM)	135
1.5.1	ACRM Corrosion Rate Sensors	135
1.5.2	ACRMDL Field Installation	137
1.5.3	Field Site Operation	137
1.6	NITRIC ACID VAPOR SAMPLING	137

APPENDIX - METHODOLOGIES

The following subsections describe the program methods and measurements in detail. Section 1.0 describes the sample preparation, exposure and damage measurement detail for each material. Because readers may be interested in only specific materials, each material is described in a stand-alone standard operating procedure content format. In Section 1.2, the damage measurements are described. After a general description of weight loss measurements, the process details for each material are given. The descriptions of strength loss measurement for nylon, appearance measurement for paints, and polymer damage measurement include the details for the materials. The remaining subsections are also in stand-alone format.

1.0 MATERIAL SAMPLE PREPARATION, COMMON METHODOLOGIES

Sample specimen preparation, exposure procedures and damage measurements were based on the guidelines of ASTM G50-76 "Standard Practice for Conducting Atmospheric Corrosion Tests on Metals", ASTM G1-81 "Standard Practice for Preparing, Cleaning and Evaluating Corrosion Test Specimens", ASTM D-1682 "Breaking Load and Elongation of Textile Fabrics", and specific material procedures developed in EPA programs. Where required, the above procedures were modified or additional standard operating procedures were developed.

Duplicate samples of all materials were exposed at each field site for all exposure periods and for each laboratory experiment. Due to cost and site space constraints, samples were limited to duplicate sets, with the exception of concrete, which had triplicate sets (because of anticipated high variation of weight loss between individual specimens). Duplicate samples provide a measure of the precision of damage measurements as well as a back-up if one sample became invalid. (Hereafter, samples imply duplicate samples).

Standard specimen size was 10.16 cm x 15.24 cm (4 in by 6 in) with varying thicknesses for rigidity. They were generally cut from sheetstock. As described below, polyethylene, concrete and nylon specimens required a different specimen size. Specimen dimensions provided a maximum surface area with sufficient strength to withstand high wind and other exposure and handling stress. All weighed samples had a mass less than 200 grams, the maximum capacity of the analytical balance used in this program.

All specimens except concrete were marked by a unique identification numbering system consisting of punched or drilled holes readable from one side only. The punched hole system is shown in Figure A-1. Concrete specimens had an identification number painted on the bottom facing side.

All similar looking materials had a unique number set for identification.

All specimens were cleaned prior to deployment and handled with gloves throughout the cleaning process. The cleaning procedure varied with the material type. Oil, grease, fingerprints, ink marks, and other contaminants were removed from all material specimens. All material specimens were stored in a temperature and humidity controlled weighing room (20 - 21^{o}C and 35 - 45% RH) for a prescribed time period. Specimens were weighed to 0.0001 grams on a digital analytical balance in the weighing room. An 80 gram standard was weighed periodically as a quality control (Q.C.) check and randomly selected specimens reweighed as an additional Q.C. check. The balance was routinely calibrated prior to weighing samples. After weighing, each material specimen was individually sealed in a plastic bag and stored in darkness in a cardboard box.

Most materials for preparing samples were obtained locally with the exceptions being nylon, obtained from a United States manufacturer and galvanized, nonchromated iron obtained through CARB.

(EDGE CLIPPED ONLY ON #90 AND #99 FOR ORIENTATION)

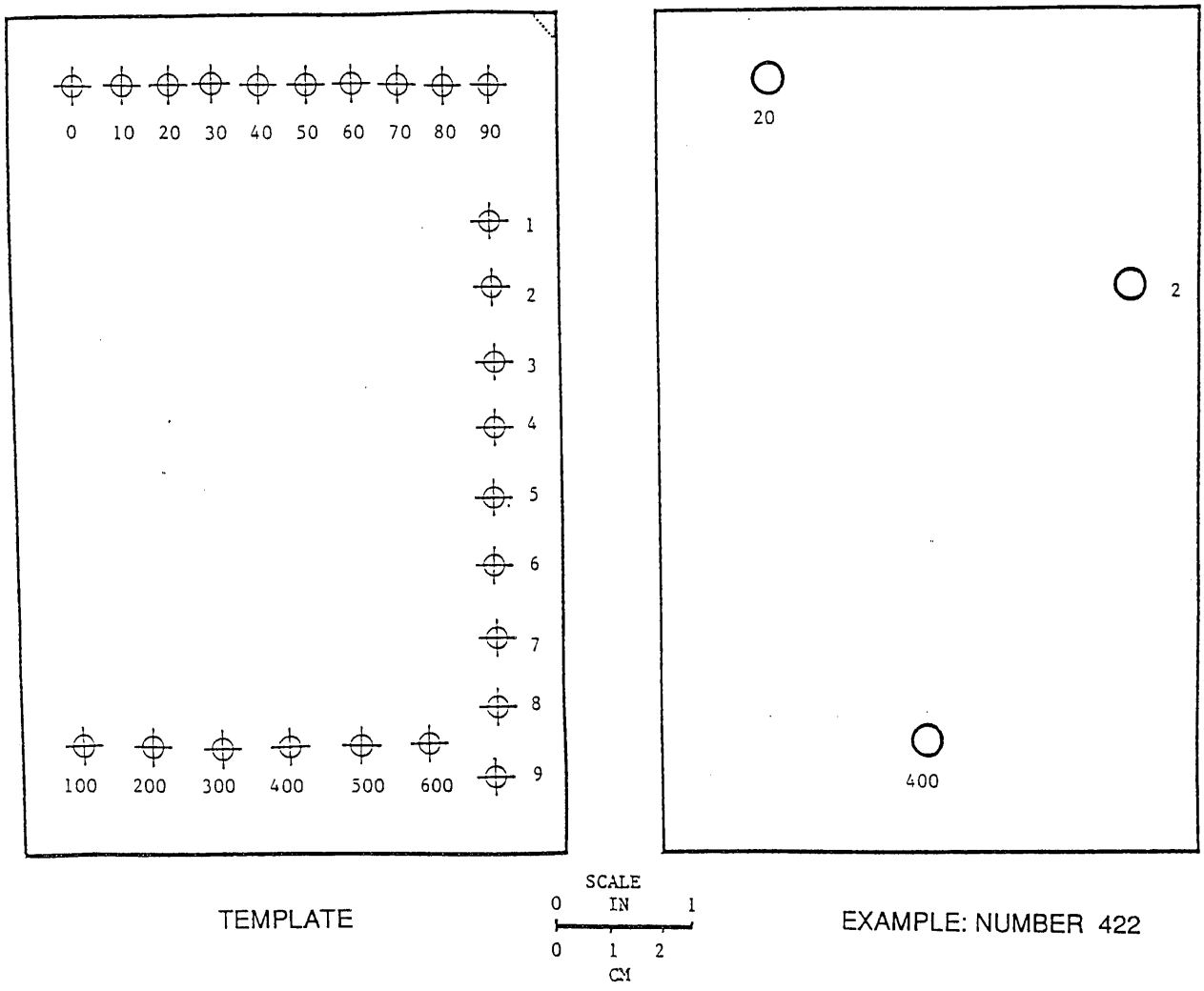

FIGURE A-1. SPECIMEN IDENTIFICATION NUMBERING SYSTEM (PUNCHED HOLES)

Immediately following deployment all specimens were re-stored in light excluding cardboard boxes in the weighing room. All extended program samples slated for weight loss analysis were weighed before and after damage measurement processing, for corrosion products and for process monitoring. Processing was done in batches by sample recovery dates, with field and/or process blanks included in each batch. All samples were inspected in the field and laboratory prior, during, and after exposure and processing, with any irregularities noted.

1.1 PREPARATION OF MATERIALS, MATERIAL SPECIFIC

The following is a detailed description of the sample preparation procedure for each material.

Nickel

Nickel 200, 24 gauge, was sheared to 15.24 cm x 10.16 (6 in x 4 in) plates by the local supplier. Identification holes were punched after initial inspection and degreasing. After deburring any sharp edges, the specimens were cleaned with detergent and water and handled with gloves. Acetone was used to remove remaining organic material including permanent ink marks and fingerprints. The specimens were given a final rinse with deionized water, dried, equilibrated for 24 hours, weighed, packaged in individual bags and stored in light excluding cardboard boxes in the weighing room.

Galvanized Steel

Electrogalvanized, nonchromated, 24 gauge steel was sheared to 15.24 cm x 10.16 cm (6 in x 4 in) plates by the local supplier. The material specimens were inspected, degreased and identification holes were punched.

After deburring any sharp edges, the specimens were cleaned by washing with mild detergent, rinsing with acetone to remove remaining

organic material including permanent ink marks and fingerprints, and finally rinsed with deionized water. Since ungalvanized steel was exposed on the edges because of shearing and hole punching, the exposed edges were painted with a rust inhibiting primer. Paint was applied by touching the plate edge to a paint soaked pad and using a conical pad to coat the holes. While drying, the specimen was suspended from a wire hook through an identification hole. After drying for 48 hours, the specimens were rinsed with deionized water, and then equilibrated for 24 hours. They were then weighed and stored in an individually sealed bags, put into light excluding boxes, and then placed into the temperature and humidity controlled room.

Paint On Stainless Steel

Two carbonate containing paints (one high and one low) were applied to stainless steel substrate plates. Stainless steel was used since it is a nonreactive substrate enabling paint weight loss to be measured. Type 304, 24 gauge stainless steel was sheared to 15.24 cm x 10.16 (6 in x 4 in) plates by the local supplier. Holes for identification were punched or drilled in the plates, which were then deburred and cleaned to remove oil, grease and ink.

The paints were from different manufacturers, but both were vinyl acrylic interior-exterior Navajo white house paints. CARB obtained the carbonate content, in confidence, from the manufacturer. Light sanding and acid wash etching were required for paint adherence to the stainless steel. Professional painting specialists lightly sanded and acid washed the plates before spray painting with thin multiple coats; paint thickness was approximately 0.5 mills.

Painting of the stainless steel samples was done in batches with each sample uniquely numbered to eliminate any confusion over paint type. The painted samples were dried for two weeks, baked for one hour at $70^{o}C$ in a convection oven, washed, rinsed, equilibrated. They were then weighed, packaged and stored.

Paint On Wood

The same carbonate extender-free paint used above was applied to a wood substrate to obtain appearance change data for paint when applied to substrate most commonly used by the public. Wood, however, has serious substrate variables including swelling and contracting with changing ambient moisture, grain, texture including cracks and knots, and lignin deterioration from sunlight, resulting in the loosening of fibers. These variables of the wood must be considered in specimen preparation since they are capable of causing greater damage to a paint coating system than that normally encountered from exposure to air pollutants.

Procedures for wood preparation and painting were established by consultation with R. Sam Williams, Research Chemist Wood Surface Chemistry and Property Enhancement, with the USDA Forest Service, Forest Products Laboratory.

Western Red Cedar was the wood chosen due to its minimum swelling and shrinking with changing ambient humidity. All wood samples were chosen having uniform fine grain with no knots or cracks. Each wood specimen was cut for vertical grain, and planed to 10.16 cm x 16.51 cm x 1.27 cm (4 in x 6 in x 1/2 in) blocks. The specimens were kept in darkness immediately after planing to prevent lignin deterioration. Identification coding numbers were drilled approximately 0.3 cm (1/8 in) into the bottom face. Painting of the wood samples was done by a professional wood products shop. Before painting, the block edges were sealed with a 50/50 mixture of commercial epoxy sealant and varnish. The top and bottom surfaces were primed with a primer recommended for Western Red Cedar; the paint was then applied by roller. The samples were dried at the shop, inspected at EMSI, and stored in a plastic bag within a light-excluding cardboard box. They were then placed within the weighing room.

Nylon Fabric

Nylon fabric specimen size and preparation procedure was developed through consultation with Dr. Chris Ladisch of the Purdue University Textile Laboratory. The fabric chosen was a nylon cloth used for the outer shells of garments and tents. A sample bolt of the fabric was obtained from the United States manufacturer, Glen Raven Mills, Inc.

Fabric Description provided by the manufacturer:

Style:	630/50
Wt-Oz/Lin Yd:	3.87 (119.20 g/m)
Oz/Sq Yd:	2.84 (95.42 g/m^2)
Yards/Lb:	4.13 (8.26 mg/Kg)
Weave:	Plain
Reed Const:	49.1, 60 x 50 (124.7 cm)
Greige Const:	46.75, 60 x 50 (118.7 cm)
Warp:	200/34/R25 Brt Nylon
Fill:	200/34 R25 Brt Nylon
	100% Nylon

This is a non-treated filament for outer shells of garments.

The following washing procedure was adopted from Purdue University procedure. Gloves were worn whenever handling the fabric. Portions approximately 3 meters (3 yards) long were cut from the bolt and prepared as follows:

1. The fabric was washed.
2. Cleaning solution was prepared with water, sodium carbonate (1 gram/liter) and non-ionic surfactant (1 gram/liter).
3. The solution was measured for a 30:1 ratio of solution to fabric by weight.
4. The measured solution was poured into a stainless steel wash basin and the fabric was immersed with the initial solution temperature at 20°C.
5. Over a period of 15 minutes the temperature of the bath was raised to 50°C.
6. The fabric was soaked for 30 minutes with constant, gentle agitation with a glass rod.

7. The fabric was then removed and rinsed first in warm tap water and immediately rinsed in cold deionized water.

8. The fabric was hung vertically to dry for 24 hours.

9. The dry fabric was loosely folded, covered top and bottom with large Kimwipes to fit into a large plastic bag, and then stored in the weighing room.

Two different specimen dimensions were used because of incompatible requirements of the field and laboratory sites, and particular damage measurement specifications.

Damage measurement by breaking strength was an essential consideration in the specimen dimensions. Breaking strength in fabrics varies with orientation. The breaking strength test required five individual strips a minimum of 3.175 cm x 17.78 cm (1 1/4 in x 7 in) long. The 7-inch dimension was the warp direction taken from the bolt length (parallel to the selvage). Additional margins were allowed for unravelling, installation, cutting loss or error, and specimen identification. The warp direction was marked since it was unclear by visual examination. The fabric was attached to a Teflon mesh screen, a nonreactive substrate, and was sewn on the installation margins using nylon monofilament line.

Field deployment on pre-installed Teflon mesh screen, often under windy conditions, required the use of staples and plastic tape to attach specimen margins to the screen.

Nylon was used during the extended program, and deployed on the field racks preexisting from the initial program. The racks (see Section 1.3) had a grid size of 11.43 cm x 22.86 cm (4 1/2 in x 9 in). For maximum space utilization, two increments of this grid were used. Thus, specimen size for meeting field use considerations was 20.32 x 22.86 cm (8 in by 9 in) with the length representing the warp direction.

The laboratory test chamber had restricted size and available space (see Section 1.4). The specimen size selected to meet the requirements was 43.18 cm x 13.97 cm (17 in x 5 1/2 in). To fit into the chamber, the fabric was installed on a Teflon mesh inverted "U" catenary-like frame. The frame was 45.72 cm (18 in) long, 17.78 cm (7 in) in catenary length, and 4.45 cm (1 3/4 in) across the base (see Figure A-2). The fabric was washed with deionized water and dried.

Specimens were cut from the washed fabric, with cutting done in the weighing room on a clean paper-covered table. The warp direction was indicated with an arrow drawn on a corner margin. Specimens were immediately identified by installing eyelets in a unique numbering pattern on the upper margin of the fabric specimens. Master templates for the two specimen sizes are shown in Figure A-3. A pencil dot was made at the eyelet site. A razor cut "X" not exceeding 0.32 cm (1/8 in) was made at the spot. The eyelet was installed by placing the lower eyelet half on a needle point cone to open the gap in the fabric and allow the eyelet to go through without snagging or stressing the fabric. The specimen number was written on the upper left margin for convenience, but the eyelet identification system was more durable. Numbered specimens were individually bagged and stored in the weighing room.

Aluminum

Aluminum 1100 series H-14, 0.0508 cm (0.020 in) thick was sheared to 15.24 x 10.16 cm (6 in x 4 in) plates by the local supplier. The specimens were washed to remove oil, grease and ink marks. The standard punched hole numbering system was used. Since anodized aluminum was used on the related acid fog study (CARB Contract A5-138-32), and anodized aluminum and nonanodized aluminum appear similar, different number set intervals were used for the two aluminum types.

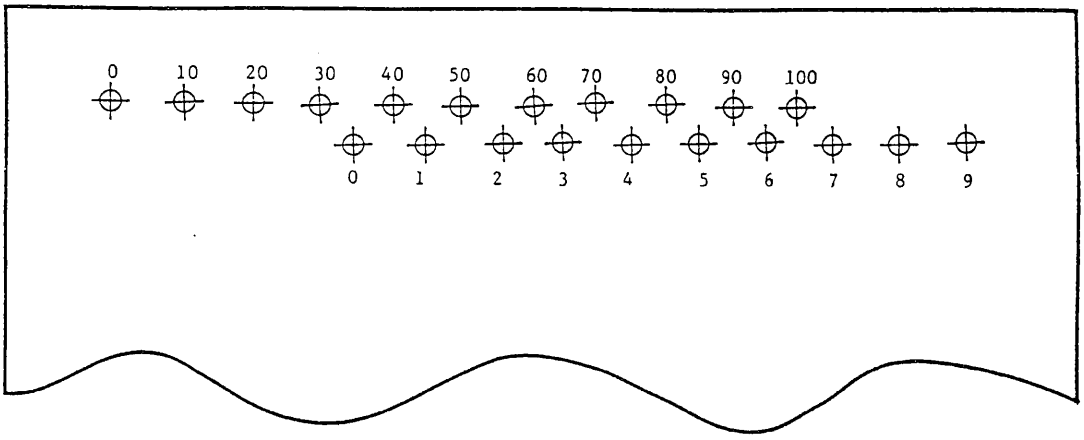

FIGURE A-2a. TEMPLATE FOR NYLON FABRIC SPECIMENS PREPARED FOR FIELD SITES (UPPER PART OF SPECIMEN).

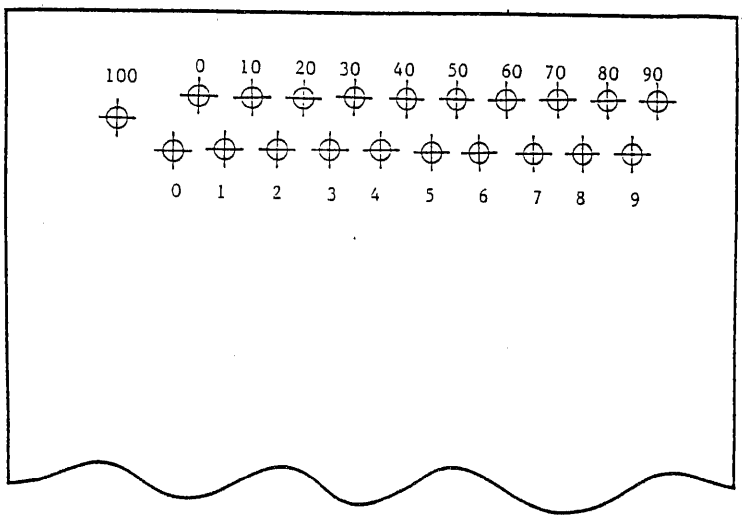

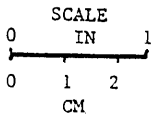

FIGURE A-2b. TEMPLATE FOR NYLON FABRIC SPECIMENS PREPARED FOR LABORATORY TESTS (UPPER PART OF SPECIMEN).

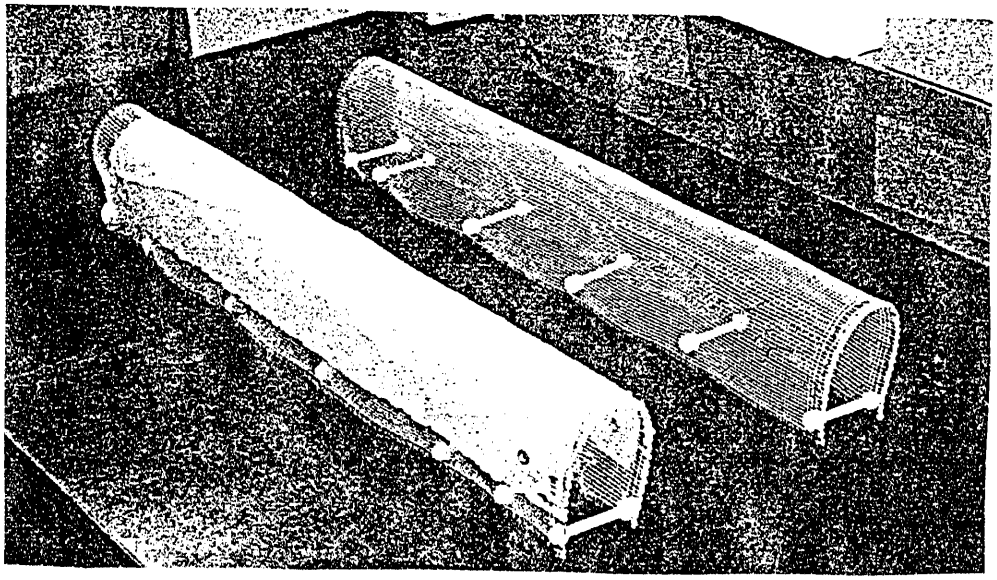

FIGURE A-3. NYLON FABRIC AND TEFLON MESH FRAME FOR LABORATORY TESTS.

Aluminum specimens were degreased with acetone, washed with detergent and water, rinsed with deionized water, and dried. The aluminum specimens prepared before October 1987 were not weighed due to a misunderstanding in processing procedure. Specimens prepared after October 1987 were weighed. All aluminum specimens were stored in individually sealed plastic bags in the weighing room.

Polyethylene

High density polyethylene (HPDE) of 0.32 cm (1/8 in) sheet thickness was cut into 13.34 cm x 15.24 cm (5 1/4 in x 6 in) size plates for field deployment by the local supplier. This size provided a margin for installation of the field rack with nylon bolts. For laboratory use the specimens were the standard 10.16 cm x 15.24 cm (4 in x 6 in size) with the saw cut made from the underside. Identification holes were drilled using the standard 10.16 cm x 15.24 cm (4 in x 6 in) size numbering template and centering on it the 13.34 cm (5 1/4 in) wide specimens. The polyethylene specimens were wiped with Kimwipes, washed in mild detergent, rinsed with deionized water and dried. They were then sealed in individual plastic bags and stored in light excluding boxes in the temperature and humidity controlled room.

Concrete

Concrete specimens were cut using a wet masonry to 3.81 cm x 3.81 cm x 10.16 cm (1.5 in x 1.5 in x 4 in) from locally obtained concrete building bricks. Loose aggregate was brushed off with a nylon brush. Specimen dimensions provided a specimen weight less than the 200 gram limit of the analytical balance, a high surface to volume ratio and sufficient strength to withstand shipping and handling. Identification numbers were painted on one long side. After allowing the paint to dry for 48 hours, the concrete specimens were washed in deionized water in an ultrasonic cleaner for 30 minutes, dried for 6 hours at 70^{o}C, equilibrated for 24 hours. They were then weighed and placed individually into labeled heavy duty, sealable plastic labeled bags.

The bagged samples were then weighed and stored. Weighing in the bag was done to include and capture any loose aggregate.

1.2 DAMAGE MEASUREMENT OF MATERIALS

1.2.1 Weight Loss Group

Weight loss is the primary damage measurement parameter for galvanized iron, nickel, concrete, aluminum and paints on stainless steel. Included in this section is a general description of the weight loss measurement process.

Weight loss is calculated as the initial predeployment specimen weight minus the final post corrosion removal weight and a field blank correction value. If the specimen lost weight, the sign is positive. Field blanks are material specimens prepared and processed identically to the other specimens and transported, installed and immediately removed from field sites. Field blank exposure time is zero. The weight loss equation is:

$$W = W_i - W_f - (\Sigma W_{bi} - \Sigma W_{bf})AVG$$

where:

W = Weight loss of the material specimen
W_i = Weight of prepared specimen before deployment
W_f = Weight of specimen after corrosion product removal
W_{bi} = Weight of field blank specimen before deployment
W_{bf} = Weight of field blank specimen after corrosion of product removal
$(W_{bi} - W_{bf})AVG$ = Average weight loss of field blank specimens

All material specimens for weight loss measurement underwent three phases of post deployment processing.

1. Documentation. The specimen was described and photographed as returned from the field.

2. Rinse. The specimen was rinsed in deionized water. An option in the original program was to analyze the rinse for cations and anions. Although this option was dropped early in the program, the rinse procedure was continued to maintain processing consistency. The rinse phase of processing was material specific.

3. Removal of corrosion products. Corrosion products were removed by immersion in a descaling solution which was material specific. The material specimen was rinsed, dried, equilibrated and weighed. Unusual contaminants such as bird droppings were removed with care to avoid damaging the specimens.

The steps of the first phase applied to all material types and are listed below:

1. The Specimen I.D. number was verified and the specimen was inspected for unusual contamination or damage. Comments were recorded.

2. Front and back photographs were taken of all specimens from the expanded/extended program and selected specimens from the initial program.

3. A preprocessing and precleaning weight was obtained for processing analysis. This was done for selected initial program specimens and all specimens of the expanded/extended program.

4. Loose dirt was brushed off with a nylon brush (except nylon fabric).

Nickel

Nickel specimens were cleaned and rinsed in an ultrasonic cleaner. This initial rinse was for optional chemical analysis.

Nickel corrosion product removal follows Section 7.1 of the ASTM G-1-81. In general, the process is:

1. Prepare HCl solution (250 ml DI water + 250 ml HCl)
2. De-aerate the HCl solution with N_2
3. Immerse the nickel specimen for 90 seconds at room temperature (specimen rests on glass beads)
4. Immediately dry the specimen with oil-free compressed air.

The specimen was equilibrated in the temperature and humidity controlled room for 24 hours and the final weight was obtained.

Galvanized Steel

Galvanized steel specimens were rinsed and cleaned in an ultrasonic cleaner using the same method as for nickel processing.

There are several methods of corrosion product removal reported in the literature. We experimented and adapted a dual process.

1. Ammonium Acetate

Each galvanized steel specimen was immersed in saturated ammonium acetate solution (ph7) for 120 minutes (specimen rested on glass beads). The specimen was then rinsed with deionized water, dried immediately with oil-free compressed air, equilibrated and weighed. This weight was taken for a process check and was not the final weight.

2. Chromic Acid

Processing with chromic acid is a standard method; however, because of the extremely toxic and carcinogenic status of chromic acid (hexavalent chromium), its use was minimized and used only when no

other alternative was acceptable. Chromic acid solution was made up in small batches (30 gm of chromium trioxide in 150 ml deionized water). Strict measures were taken to prevent personal exposure, to properly process, totally contain, and appropriately dispose of the hazardous compounds.

Each galvanized steel specimen was immersed for 60 seconds in chromic acid solution heated to $80^{o}C \pm 5^{o}C$. The specimen rested on a layer of glass beads while immersed, and then immersed for a couple seconds through a series of deionized water rinse pans. The pans were used to totally contain and minimize the rinse water. Chromic acid is visibly yellow, coloring very dilute solutions. The final rinse pan was observed to be colorless after the rinse. Any visible yellow caused another rinse pan with fresh deionized water to be used. The final rinse was with fresh deionized water from a wash bottle. The runoff was collected in the final rinse pan.

The galvanized steel specimen was immediately dried with oil-free compressed air, equilibrated in the weighing room for 24 hours and the final weight obtained.

Aluminum

Aluminum specimens were rinsed (only for cleaning) prior to corrosion product removal. The cleaning was done with a dishwasher shower of deionized water for two minutes on each side; the rinse water was not saved for chemical analysis. As described previously, weight loss measurement by corrosion product removal was applied after October 1987.

Corrosion products were removed as follows:

1. A one batch solution of chromic and phosphoric acid was prepared (using hexavalent chromium hazard procedures) by adding 10 ml of

phosphoric acid to 190 ml of deionized water followed with 4 g of chromium trioxide.

2. Each aluminum specimen was immersed in the solution and heated to $90^{o}C \pm 5^{o}C$ for 7 minutes. (The specimen rested on glass beads).

3. Each specimen was immersed for a couple of seconds through a series of deionized water rinse plans until the last rinse showed no yellow color. It was then given a final rinse from a wash bottle with runoff collected in the last rinse pan.

4. The separate aluminum specimens were immediately dried with oil-free compressed air, equilibrated in the weighing room for 24 hours, and weighed.

Paint on Stainless Steel

Paint adherence to stainless steel was too weak for ultrasonic cleaning. Instead, an agitator was used for the initial rinse (to produce a rinse for optional chemical analysis). The agitator was run at 80 cycles per minute for 30 minutes. Due to possible paint damage from glass beads, pans with corrugated bottoms were used. The painted specimen plates were turned over halfway through the rinse cycle. After the agitation cycle the specimen was removed, rinsed with deionized water, and dried.

The corrosion product removal process must also be gentle not exceeding paint adherence strength. The painted specimen was gently washed in a solution of mild nonionic surfactant and water at room temperature and then wiped three times with a cellulose sponge. Each specimen was rinsed with deionized water, dried at $70^{o}C$ for one hour, equilibrated in the weighing room for 24 hours and weighed.

Concrete

Concrete specimens were cleaned and rinsed in the ultrasonic cleaner. The concrete specimen was placed in a plastic pan slightly larger than the specimen and 80 ml of deionized water was added. The pans were placed in the ultrasonic cleaner water bath and held in place with supports; the ultrasonic cleaner was run for 15 minutes; the specimen was then turned over and the ultrasonic was run for another 15 minutes; the ultrasonic rinse was for optional chemical analysis. This 30-minute process also served as the corrosion product removal phase. The specimen was rinsed in fresh deionized water and oven dried for 6 hours at 70°C. After equilibration a final weight was obtained.

Strength Loss For Nylon Textile

Breaking strength (load) of the control and exposed nylon fabric specimens was carried out according to ASTM D-1682 with an Instron Universal Testing Instrument Model 1130 (Instron Corporation, Canton, Massachusetts), a constant-rate-of-extension tensile testing machine. All fabric specimens were conditioned at 21°C and 65% RH for at least 48 hours prior to testing. A minimum of five warpwise raveled strips from each fabric specimen was tested.

ASTM D-1682 provides options of test method, option 1R 2.54 cm (1 in) raveled strip test was selected for the type of specimen and option E (constant-rate-of-extension) was selected for type of testing machine.

The laboratory test specimens were removed from the Teflon frames at EMSI. The field specimens were removed from the Teflon frames at the field sites, loosely folded into Kimwipes, and placed into plastic bags. The field specimens were unpacked at EMSI and exposed in the weighing room. Some field specimens were damp when recovered because of recent rain but exposure in the weighing room allowed the specimens to dry. All specimens were repackaged in the weighing room into clean, plastic bags with Kimwipes to prevent direct contact of nylon and plastic. The

specimens were packaged and sent to Dr. Chris Ladisch of the Purdue University Textile Laboratory.

1.2.2 Appearance Measurement

Appearance damage measurement was done with a colorimetric methodology analyzing for color and luster change. The methodology included pigmentation change analysis.

Appearance change measurement was the primary damage measurement parameter for paint on a wood substrate; it was a secondary measurement for paint on a stainless steel substrate. Colorimetric industry subcontractors performed the measurements and analysis on the specimens. The painted specimens were then shipped to the subcontractor's facility for measurements.

1.2.3 Polyethylene Damage Measurements

Processing was not performed because the simple, inexpensive method for determination of corrosion damage was not available.

1.3 FIELD EXPOSURE RACKS

The field exposure racks were based on the design specifications of ASTM G50-76. The rack frame was made of slotted galvanized angle iron. The exposure plane sloped at a 30^{o} angle from the horizontal and faced true south. All material specimens were at least 1.2 meters (4 feet) above the ground, roof surface or other obstructions. All sites are above gray-white crushed-rock-covered roofing paper or gravel-covered ground. Figure A-4 shows the rack at the Upland site. Figure A-5 is a diagram of rack design. The racks were designed to accommodate up to 140 material specimens in 11.43 cm x 22.86 cm (4 1/2 in x 9 in) size spaces. Material specimens of 11.43 cm x 15.24 cm (4 in x 6 in) size were held in place with porcelain insulators as illustrated in Figure A-4. The 11.43 x 15.24 cm (4 in x 6 in) material specimens included

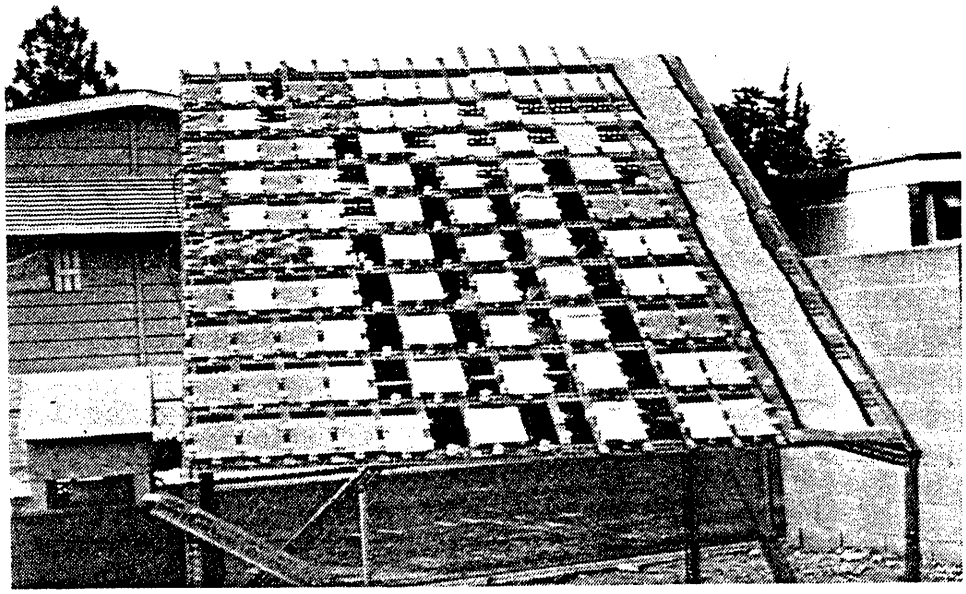

FIGURE A-4a. FIELD SITE PHOTOGRAPH OF SPECIMEN RACK, UPLAND.

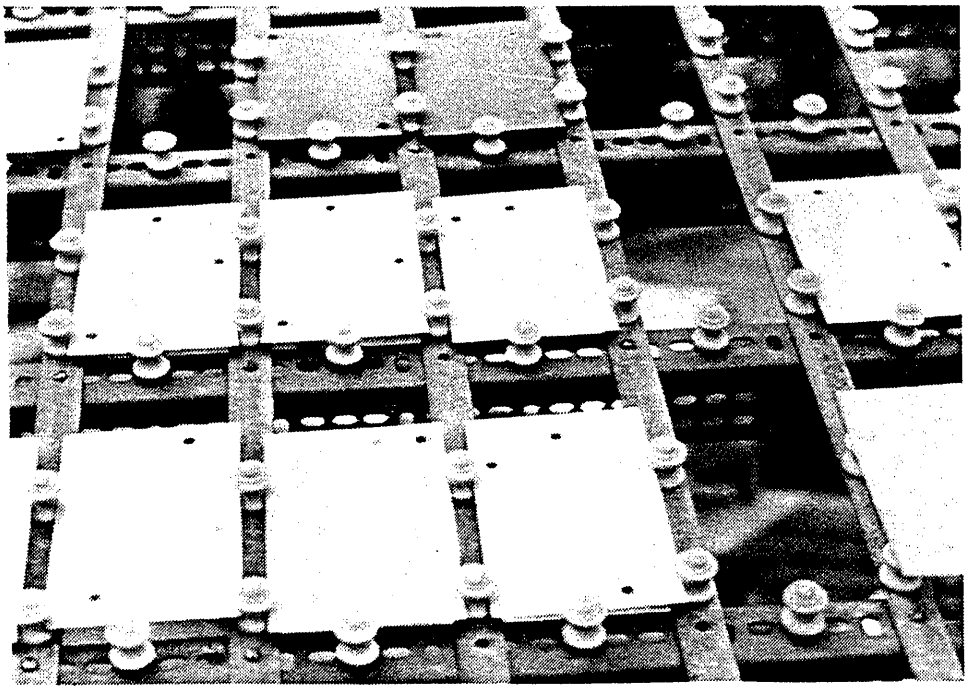

FIGURE A-4b. CLOSE UP OF SPECIMEN RACK.

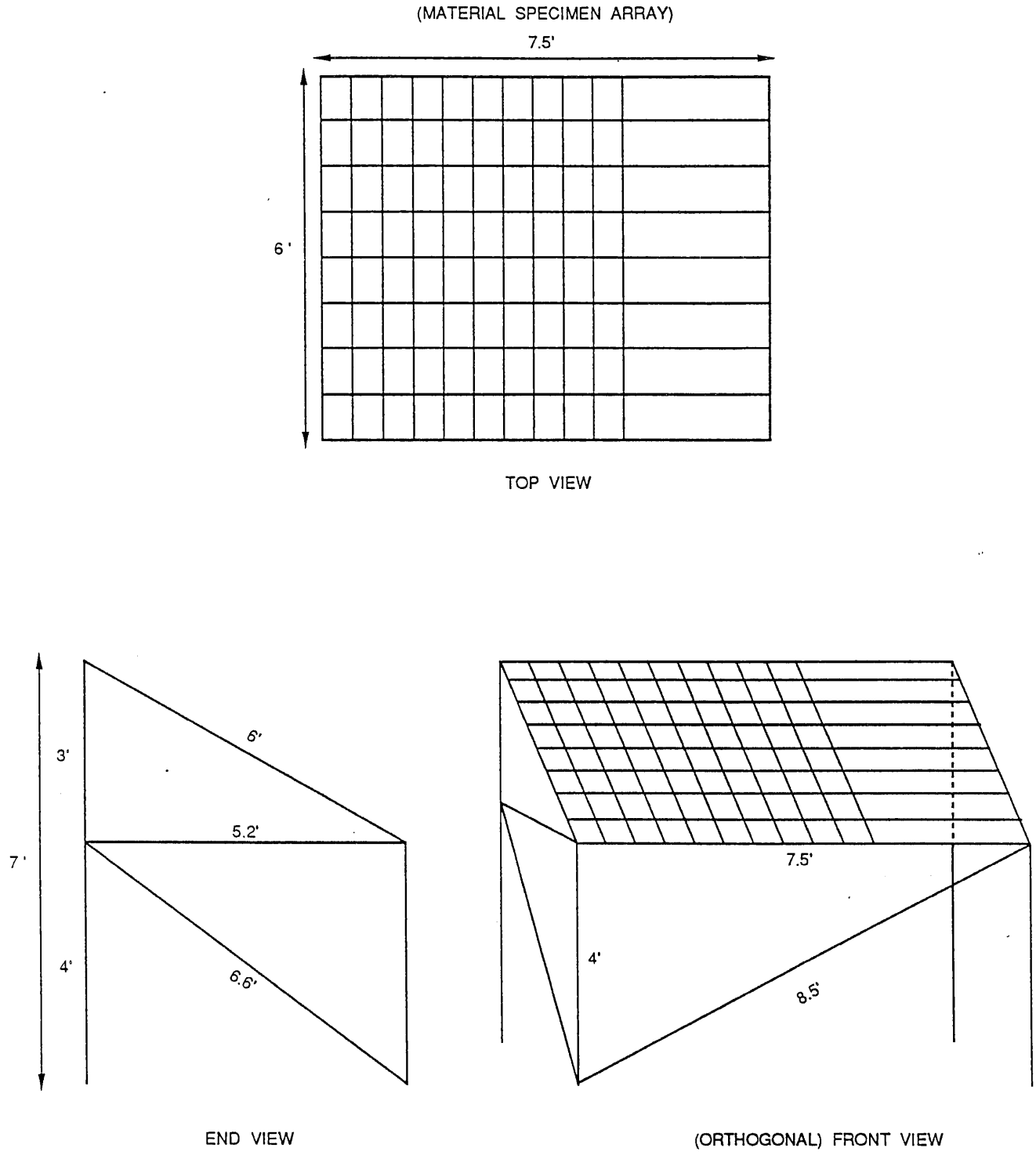

FIGURE A-5. FIELD SPECIMEN RACK DIAGRAM

nickel, paint on stainless steel, aluminum, concrete material when installed on plates, and the ACRM sensors when installed on plates. The concrete specimens were installed in the field; they rested on a nylon frame bolted to a 11.43 x 15.24 cm (4 in x 6 in) galvanized steel plate. The porcelain insulators and nylon hardware prevented galvanic corrosion.

Painted wood specimens were too thick for the porcelain insulators. They were installed within soft plastic tube rollers resting on nylon washers.

High density polyethylene was bolted above the rack with a porcelain insulator used as a spacer. Nylon bolts and washers were used.

The nylon fabric was attached to the Teflon screen as described in Section 1.1. The Teflon screen was bolted to the frame using a nylon bolt and porcelain insulator as a spacer.

1.4 LABORATORY TESTS

In the laboratory tests the same materials and the ACRMs sensors exposed at the four field sites were exposed to atmospheres of carefully controlled concentrations of pollutants for periods of 28 days/test. In each test a 6 hour (h) cycle consisting of 1.5 h at 16^{o}C and 4.5 h at 22^{o}C was used. A cooling cycle was used to induce condensation at the sample surface.

In the initial program, the laboratory tests were conducted at the Rockwell Science Center. In the expanded/extended program, the tests were conducted at the University of Southern California.

A detailed description of the test procedure follows.

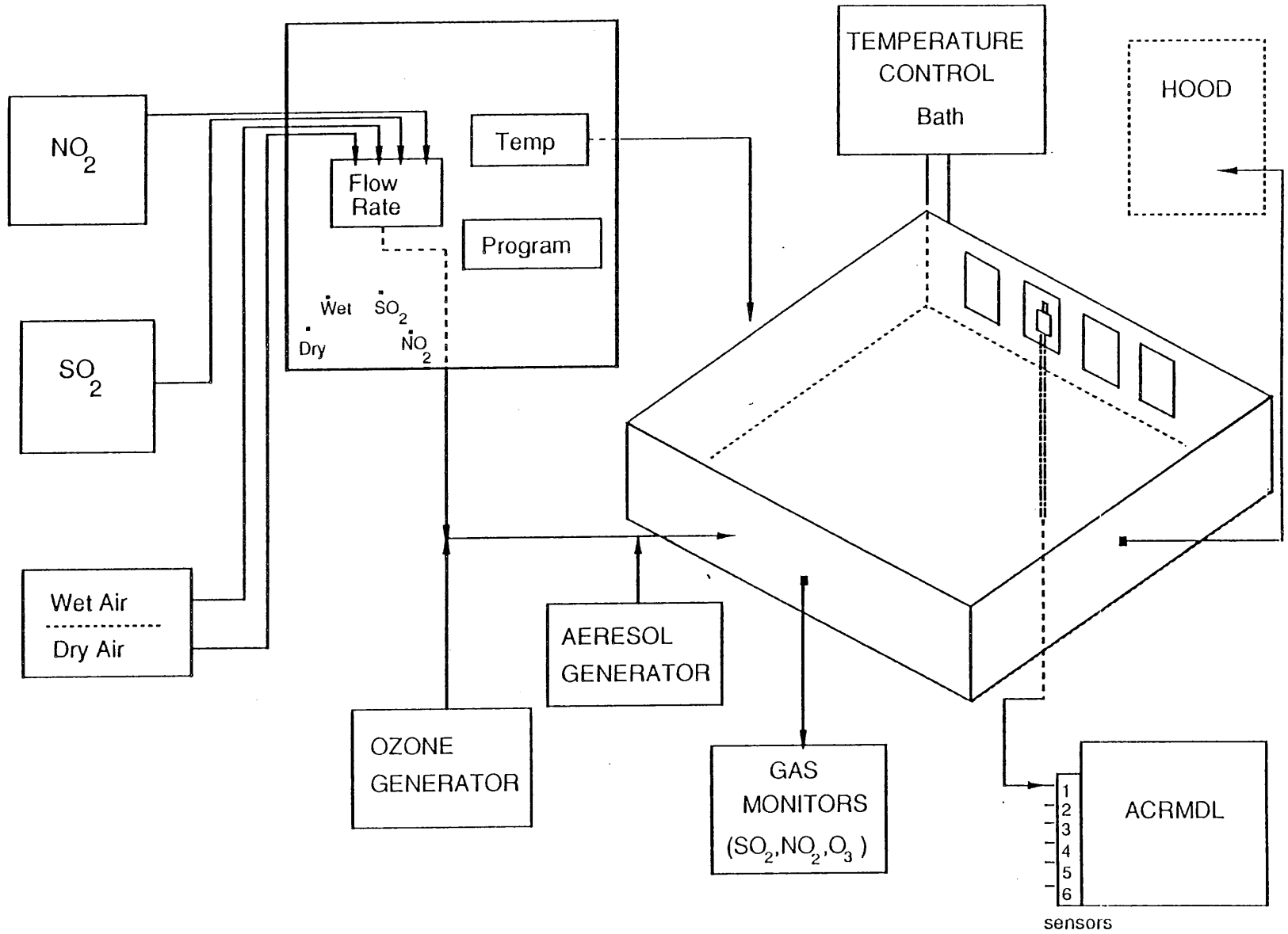

FIGURE A-6. LABORATORY ACID DEPOSITION CHAMBER

The aerosol generator was a 500 cm^3 micronebulizer. Aerosol was generated by nebulizing an 8 mM HNO_3 solution at a flow rate of 8 l/min. and introducing it into the test chamber. Nominal HNO_3 concentrations of 0.5 and 0.1 ppm were used.

The Test Chamber

The test chamber used was a rectangular shaped housing the interior of which was Teflon-coated. Samples were attached to the walls which have room for four 10.2 cm x 15.2 cm coupons/per wall, one of which was an ACRM sensor mounted on a nickel or galvanized steel coupon. All inlets and outlets for gases and the ACRM leads were located at the bottom of the test chamber. A fan in the shape of a three-blade propeller was used to ensure uniform distribution of the pollutants in the test chamber. The test sequence consisted of a 6 h cooling/heating cycle, thermoregulated by a TE-8J Tempette thermoregulator in a Techne bath. The cover of the test cell was made of clear plastic which allowed visual observation of the samples during the test.

1.5 ATMOSPHERIC CORROSION RATE MONITOR (ACRM)

The atmospheric corrosion rate was monitored with an Atmospheric Corrosion Rate Monitor Data Logger (ACRMDL) manufactured by Sunset Laboratories. Nickel and zinc sensors were installed on nickel or zinc material specimens, respectively, at EMSI. The systems were installed at field sites by EMSI and installed at the laboratory test chambers by the operators.

1.5.1 ACRM Corrosion Rate Sensors

Nickel and zinc sensors were obtained from the manufacturer. A detailed description of the sensors is given in a report by F. Mansfeld (9). At EMSI the loads were sprayed with plastic for weatherproofing, installed on material specimen plates of the same metal, and then fastened with nylon screws. Figure A-7 shows an ACRM sensor installed

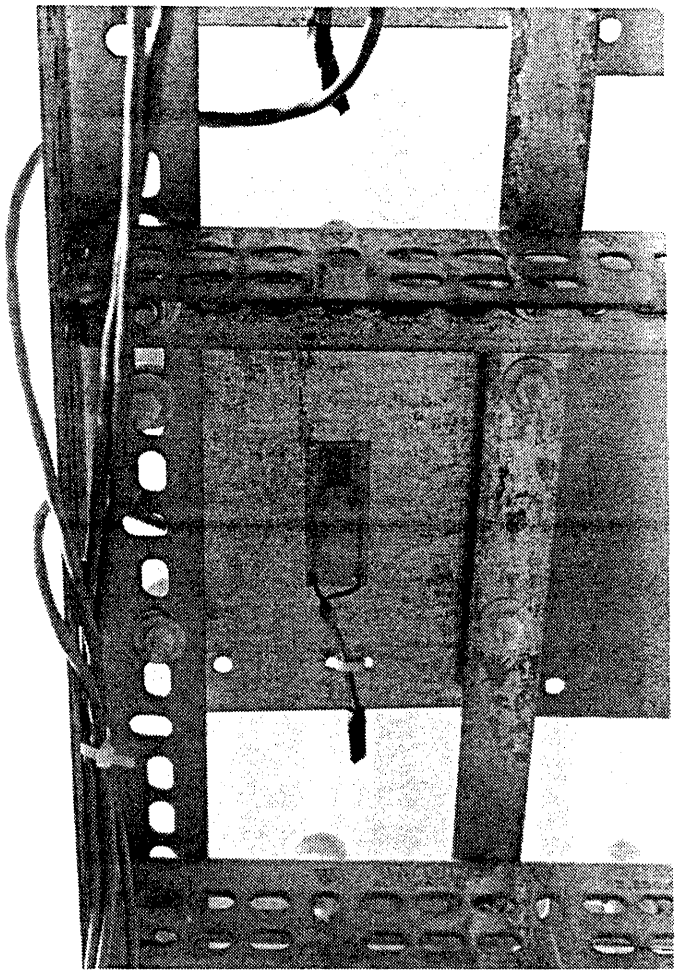

FIGURE A-7. ACRM SENSOR INSTALLATION ON A FIELD SPECIMEN RACK, (FACE DOWN).

on an exposure rack.

1.5.2 ACRMDL Field Installation

The ACRMDL was housed in a weatherproof case and initially installed in a 61 cm x 61 cm (2 ft x 2 ft) box attached to an edge of the specimen rack. Since there were problems with condensation and water entry into the ACRMDL case, the systems were moved indoors later in the program.

1.5.3 Field Site Operation

Site operators changed and inspected paper data on the ACRMDL tapes during the installation of a HNO_3 vapor filter approximately every six days. If the site operator noted a malfunction, EMSI was called. Some malfunctions could be solved by the site operator with consultation over the telephone. If required, EMSI staff would visit the site and reprogram, repair or remove the ACRMDL for factory repair. EMSI supplied each site with microcassette tapes, paper tapes, printer ribbons, data log forms and mailing envelopes. The site operators mailed the cassettes with the paper tape back to EMSI in individual mailing envelopes. Each microcassette and paper tape was inspected upon arrival at EMSI. During the project, microcassette reading and data processing was performed at RISC, USC and EMSI.

1.6 NITRIC ACID VAPOR SAMPLING

HNO_3 vapor sampling was conducted as part of this project at each field site and was performed with a two-stage filter pack containing 37 mm Teflon and nylon filters. The Teflon filter was placed upstream of the nylon filter to remove particles. HNO_3 vapor was captured on the nylon filter commercially manufactured for HNO_3 vapor collection. The nylon filter rested on a support pad.

At each field site the filter was installed in a sampler attached to the material specimen exposure rack. The system was contained in a HIVOL type frame with the inlet at the average height of exposed material specimens. The system consisted of a critical orifice for a 4 l/min flowrate, a pressure gauge, a rotameter, and an electric pump controlled by a standard HIVOL timer. The site operator installed and removed the filter packs on the work day before and after the date specified by the California particulate 6-day interval sampling schedule.

The filters were packaged at EMSI in monthly batches. They were numbered, sealed with plugs and enclosed in plastic bags, then shipped to the field sites in coolers with gel ice packs for return shipment. The site operator maintained a logbook noting the filter identification number, gauge readings and remarks. The site operator replugged, bagged and refrigerated the filter immediately. Exposed filters and randomly selected field blanks were shipped to EMSI by the site operators approximately every month. The filters were logged in and immediately refrigerated until analyzed.

The analysis procedure for HNO_3 filters is described below.

- Gloves were worn during all handling procedures. Beakers used for extraction were cleaned and oven dried before use.

- The nylon filters were extracted in a 0.003M $NaHCO_3$/0.0024M Na_2CO_3 solution which was also the working eluent for the Dionex Ion Chromatograph.

- For each filter, 10 ul of eluent was added to a clean 100 ml beaker using a calibrated repipette. The nylon filter was then placed exposed side down in the extraction solution. The beakers were immediately covered with parafilm and extracted ultrasonically for 30 minutes.

- A reagent blank was prepared for every 20 or fewer samples. This was done by adding the eluent to a beaker not containing a filter; it was extracted along with the samples. The purpose was to monitor the extraction blank levels.

- A 25 ug/filter NO_3^- filter spike was also prepared for every 30 or fewer samples by adding 25 ul of a 1000 ug/ml NO_3^- quality control stock solution to a blank filter and then extracting along with the regular samples. This was to check on the extraction and analysis.

- The extracts were then analyzed with a Dionex Ion Chromatograph. A calibration curve (standards ranging from 25.0 mg/l NO_3^- to 0.10 mg/l NO_3^-) was run at the beginning and end of sample run or after every 30 samples, whichever was more frequent. Working standards were made fresh daily from a stock solution prepared fresh every 6 months. After each standard curve and after every 10 samples, a Quality Control Check Sample (QCCS) was analyzed. The percent recovery for the QCCS when compared to the standards was required to be within 95-100%. The QCCS was made fresh from separate stock solution other than the one used to make up the standards.

- The standards and samples were loaded onto an autosampler tray and analyzed using an automated injection system. An electronic integrator was used for recording the ion chromatographic peaks with a strip chart backup. The instrumental responses were then automatically transferred to the computer. Laboratory results for NO_3^- were stored in the computer files as ug/ml in filter extent. The values were then converted to ug/filter, using the following equation:

$$\text{Micrograms of } NO_3^-/\text{filter} = (\text{ug } NO_3^- \text{ ml})(\text{volume of extract})$$

An extract was analyzed in duplicate for every 20 or fewer samples.